water

MDPI

Article

Mitigating Long-Chain Fatty Acid Inhibition in Anaerobic Digestion of Model LCFA Substrates with *Ruminococcus flavefaciens* Bioaugmentation

Chundong Wu, Jinku Liu, Sijian Wang, Zhanbin Guo * and Chenxi Li *

College of Engineering, Heilongjiang Bayi Agricultural University, Daqing 163319, China; hbau192902@163.com (C.W.)
* Correspondence: hbaugzb@163.com (Z.G.); chenxili_byau@sina.com (C.L.)

Abstract

Anaerobic digestion of high-lipid waste possesses substantial biomethanation potential. However, its stability is readily inhibited by the accumulation of long-chain fatty acids (LCFAs). In this study, pure stearic acid and oleic acid were employed as model LCFA substrates to simulate LCFA inhibition conditions, and the mitigation effects of *Ruminococcus flavefaciens* (*R. flavefaciens*) bioaugmentation on LCFA inhibition were systematically evaluated; metagenomic analysis was conducted to analyse metabolic processes. The results demonstrated that a 1% (*v*/*v*) *R. flavefaciens* addition increased cumulative methane yield by up to 270.9% compared to the LCFAs-only reaction. *R. flavefaciens* addition was associated with enhanced LCFA conversion and promoted acetate formation. Metagenomic analysis suggested shifts in microbial community abundance, with modest increases in β-oxidation-associated *Syntrophomonas* and the acetotrophic methanogenic archaeon *Methanosarcina*. Analysis of metabolic pathway-related enzyme genes revealed that *R. flavefaciens* addition was associated with higher abundance of key genes involved in LCFA activation, β-oxidation, and acetate-utilising methanogenesis, potentially contributing to putative LCFA conversion, alleviating LCFA inhibition. Concurrently, carbohydrate-active enzyme analysis revealed that *R. flavefaciens* addition elevated glycosyltransferase and carbohydrate esterase potentials associated with extracellular polysaccharide synthesis and substrate deacetylation, which may enhance substrate accessibility and biofilm formation, thereby sustaining metabolic continuity.

Keywords: bioaugmentation; long-chain fatty acid inhibition; anaerobic digestion; metagenomic analysis

Check for updates

Academic Editor: Josep Ribes

Received: 31 August 2026
Revised: 30 September 2026
Accepted: 5 October 2026
Published: 9 October 2026

Copyright: © 2026 by the authors. Licensee MDPI, Basel, Switzerland. This article is an open access article distributed under the terms and conditions of the Creative Commons Attribution (CC BY) license.

1. Introduction

Compared with carbohydrates and proteins, lipids can significantly improve the methane yield of anaerobic digestion [1–3]. Long-chain fatty acids (LCFAs) are the key intermediate products of lipid hydrolysis during lipid anaerobic digestion. When the hydrolysis rate of lipid is faster than the β-oxidation rate of LCFAs, LCFAs will continue to accumulate [4]. The accumulated LCFAs are adsorbed on the surface of microorganisms, which destroys the integrity of the cell membrane and normal physiological functions. The formed dense blocking membrane will hinder material transfer and eventually lead to the inhibition and stagnation of the anaerobic digestion reaction [5,6].

Studies have shown that the addition of functional biofortifiers in the anaerobic reaction process is an important biological means to increase methane yield. Different

biofortifiers can act on lipid hydrolysis and β-oxidation of LCFAs, respectively. Under the condition of sufficient methanogenic activity, the addition of anaerobic lipolytic bacteria (*Clostridium lundense*) can enhance the lipid hydrolysis process. The syntrophic microorganisms in the system can simultaneously carry out the β-oxidation metabolism of LCFAs, consume the LCFAs produced by hydrolysis in time, avoid the inhibition caused by the accumulation of LCFAs, and thus improve the efficiency of methane production [7]. The addition of *Syntrophomonas zehnderi* or its enriched culture to the reactor can directly increase the β-oxidation degradation rate of LCFAs, effectively reduce the accumulation of LCFAs, and promote methane production [8]. The addition of *Serratia* lipid-degrading bacteria can increase the abundance of key functional genes in the lipid hydrolysis and β-oxidation pathway of LCFAs, enhance the degradation of LCFAs, reduce the accumulation of LCFAs, and increase the methane yield [9]. When a domesticated microbial consortium centred on *Syntrophomonas* and *Methanosaeta* as key functional groups is introduced, *Syntrophomonas* enhances the efficiency of β-oxidation of LCFAs, whilst *Methanosaeta* utilises the acetate produced during this metabolic process; the two species engage in mutualism via substrate coupling, thereby alleviating the inhibitory effects caused by the accumulation of LCFAs [10].

The above studies have paid more attention to the direct regulation of the mutual function of microorganisms in the anaerobic system by adding traditional microbial agents, and less attention has been paid to non-traditional strains that can directly promote the oxidative degradation of LCFAs and alleviate their cumulative inhibition.

Ruminococcus flavefaciens is a rumen-derived cellulose-degrading bacterium, but its special cell surface protein structure gives it the potential to alleviate the accumulation of LCFAs. Studies have shown that the anchored cellulosome on the surface of *R. flavefaciens* can integrate serine protease inhibitors through the adaptor protein Scaffoldin C to form a cellulose complex, which is free from degradation by extracellular proteases, thereby maintaining the stable function of the bacteria [11]. It may maintain the activity of *R. flavefaciens* for as long as possible under the attachment of LCFAs to exert its function. Other studies have also found that the basic fermentation metabolism of *R. flavefaciens* is not dependent on cellulose degradation and continues to produce H_2 and acetic acid during the metabolic process. H_2 is used as an electron donor for hydrogenotrophic methanogens, and acetic acid can be further consumed as a methanogenic substrate [12–14]. It is speculated that the H_2 produced by this strain participates in the interspecies hydrogen transfer of the system, maintains the favorable thermodynamic condition of low hydrogen partial pressure, and alleviates the inhibition of high hydrogen partial pressure on the β-oxidation of LCFAs. Although *R. flavefaciens* has the above potential advantages, previous studies have generally focused on the degradation of cellulose due to the natural properties of its cellulose-degrading bacteria. At present, whether the strain can function in lipid-rich anaerobic digestion and alleviate the accumulation of LCFAs has not been fully studied.

In this study, different doses of *R. flavefaciens* were added to the typical LCFAs (e.g., oleic acid and stearic acid) anaerobic digestion reaction batch experimental group as a bioaugmentation agent. The effect of *R. flavefaciens* on the increase in methane yield of LCFAs was quantitatively evaluated, and the changes in physical and chemical indices in different reaction processes were observed. Metagenomic analysis was carried out on metabolic processes such as β-oxidation and methanation of LCFAs and the succession of microbial communities, and the effects of *R. flavefaciens* bioaugmentation on the metabolic pathways related to anaerobic digestion of LCFAs were elucidated. Functional annotation analysis was performed through the Kyoto Encyclopedia of Genes and Genomes (KEGG) and carbohydrate-active enzyme (CAZymes) databases to elucidate changes in the abundance of related enzyme genes in the LCFAs degradation metabolic pathway. A series of

experiments showed that *R. flavefaciens* could survive and maintain biological activity in anaerobic digestion in the presence of high concentrations of LCFAs. The addition of this strain increased the supply of acetic acid in the reaction, promoted syntrophic β-oxidation, and improved the methanogenic efficiency of LCFAs.

2. Materials and Methods

2.1. Substrate and Inoculum

LCFAs, including stearic acid (C18:0, purity > 95%) and oleic acid (C18:1, purity > 95%), were purchased from Shanghai McLean Biochemical Technology Co., Ltd. (Shanghai, China). Cattle manure was collected from Lindian County, Daqing City, Heilongjiang Province and used as an inoculum for anaerobic digestion. Following collection, the cattle manure was transported to the laboratory, thoroughly homogenised, and subjected to acclimation cultivation in a manure-to-water volume ratio of 1:3.9, an optimal dilution screened from preliminary experiments that delivered a higher volumetric methane fraction in biogas than the conventional 1:4 mixing ratio. Total solids (TS), volatile solids (VS), soluble chemical oxygen demand (SCOD), total alkalinity (TA), volatile fatty acids (VFAs), carbon-to-nitrogen ratio (C/N), and ammonia nitrogen as NH_4^+-N (AN) of the inoculum were determined. Physicochemical characteristics of the inoculum are presented in Table 1.

Table 1. Physicochemical Properties of the Inoculum.

Test Items	Inoculum
TS (wt %)	12.36 ± 1.20
VS (wt %)	7.86 ± 0.04
VS/TS (%)	63.59 ± 7.20
TA (mg/L)	4586 ± 200
VFAs (mg/L)	218.59 ± 15.65
C/N	13.57 ± 0.65
SCOD (mg/L)	17,050 ± 826.14
pH	7.27 ± 0.01
AN (mg/L)	711.83 ± 5.01

2.2. Preparation and Preservation of R. flavefaciens

R. flavefaciens was procured from Ningbo Tesuto Biotechnology Co., Ltd. (Ningbo, China). Prior to use, the glycerol stock (Deutsche Sammlung von Mikroorganismen [DSM] 25089) was thawed in an anaerobic environment and subsequently cultured in 2% (volume per volume [v/v]) rumen fluid medium (DSM 436) for 2–3 days. The culture was centrifuged at 5000 revolutions per minute (rpm) for 5 min; the cell pellet was collected and resuspended in reduced anaerobic buffer (DSM 436 base). Concentration was determined by comparison with a McFarland standard tube. *R. flavefaciens* was stored at 4 °C for 3 days at a concentration of 10^8 colony-forming units (CFU)/mL before use. This low-temperature storage was employed to slow down microbial metabolism, reduce substrate consumption and metabolite accumulation, thereby maintaining cellular stability and preventing premature senescence or loss of activity of the anaerobic strain before the experiment, ensuring consistent activity and physiological status at inoculation. The strain was cultivated using DSM436, which contains tryptone, yeast extract, glucose, cellobiose, complete mineral salts, and essential fatty acids; this nutritionally balanced formulation fully supports the survival and viability of *R. flavefaciens*, and at 4 °C, the metabolic rate of the strain was significantly reduced while the abundant nutrients in the medium effectively maintained cell membrane integrity and enzymatic activity, ensuring stable preservation of cell activity and viable cell counts over the 3-day storage period [15]. Prior to inoculation, cell viability was determined by CFU counting, verifying that the cell concentration remained stable at approximately

10^8 CFU/mL after the 3-day storage period. No pre-warming or reactivation step was applied before inoculation; the cold-stored suspension was inoculated directly into the reactors. Although CFU counting confirmed that the viable cell concentration remained stable at approximately 10^8 CFU/mL after the 3-day storage period, CFU counts alone cannot exclude a transient reduction in metabolic activity caused by cold stress.

Quantification of *R. flavefaciens*. *R. flavefaciens* was enumerated by the plate-count method under strictly anaerobic conditions. Digestive fluid samples were serially diluted (10-fold) in reduced anaerobic buffer and plated (100 µL per plate) onto agar of *Ruminococcus albus* medium (DSM 436), containing per litre: 5.0 g tryptone, 2.0 g yeast extract, 3.0 g glucose, 2.0 g cellobiose, 40 mL mineral solution 1 (0.6% K_2HPO_4), 40 mL mineral solution 2 (0.6% KH_2PO_4, 2.0% $(NH_4)_2SO_4$, 1.2% NaCl, 0.25% $MgSO_4 \cdot 7H_2O$, 0.16% $CaCl_2$), 1.0 mg resazurin, 4.0 mL Na_2CO_3 solution, 1.0 mL fatty acid mixture (isobutyric, isovaleric and 2-methylbutyric acids), and 0.5 g cysteine-HCl·H_2O as reducing agent (pH 7.0), solidified with 1.5% (*w*/*v*) agar. Plates were incubated anaerobically at 37 °C for 2 days. Colonies with typical *R. flavefaciens* morphology were enumerated; because this medium is semi-selective, colonies were assigned presumptively. The limit of detection was 1.0×10^3 CFU/mL.

2.3. Batch Anaerobic Digestion Experiments of LCFAs

Batch anaerobic digestion was conducted in 250 mL borosilicate glass flasks with an effective working volume of 150 mL. LCFAs and inoculum were added to digestion flasks according to the ratios specified in Table 2; stearic acid was directly added as solid powder, and oleic acid was supplemented in pure liquid form, with no organic solvents, thermal melting or other pretreatment adopted for the two LCFAs throughout the entire experiment, and their actual dosing loads were 10.00 g/L (reactor effective volume) and 0.128 g/g VS (inoculum volatile solids), respectively. Excessively high LCFA loading exerts strong inhibitory effects on anaerobic microbes. LCFA concentrations $\geq$ 2 g/L induce irreversible inhibition in anaerobic digestion, and 3.5–4 g/L results in complete system destabilisation. Hence, the adopted 10.00 g/L LCFA far exceeds the tolerance threshold of anaerobic microorganisms to establish a severely inhibited model system [16]. The K (Blank) group (no LCFAs added, 0% microbial inoculum) was set as an inoculum blank to quantify endogenous methane originating solely from cattle manure inoculum. The *R. flavefaciens* suspension was not included in the VS, as the maximum amendment volume of 1.0% *v*/*v* contributed negligibly to the total solids relative to the native inoculum; instead, background methane associated with the inoculum was controlled through inoculum-only blanks [17]. All cumulative methane production presented in this study was corrected by deducting the methane production of the K group, so that the results exclusively represent methanogenesis from target substrates. Three bioaugmentation doses (0.1%, 0.5%, and 1.0% *v*/*v*) are selected for the establishment of a low-to-high gradient to evaluate dose–response relationships. A minimal inoculum is represented by the 0.1% dose, with which it is tested whether marginal exogenous input can perturb the indigenous community. An intermediate level is provided by the 0.5% dose for the identification of threshold effects. The 1.0% dose is set as the upper practical limit to achieve maximum potential metabolic enhancement via hydrogen and acetate supply, without excessive dilution of the native inoculum or overwhelming competitive pressure imposed by foreign microbes [18]. Based on the stock concentration of 10^8 CFU/mL and the effective working volume of 150 mL, the estimated initial cell densities in the reactors were approximately 1.0×10^5, 5.0×10^5, and 1.0×10^6 CFU/mL for the 0.1%, 0.5%, and 1.0% (*v*/*v*) addition levels, respectively. Prior to incubation, the flasks were flushed with high-purity nitrogen for 1 min to establish anaerobic conditions. Subsequently, they were sealed and incubated under continuous agitation at 37 ± 2 °C in a constant-temperature incubator (JDX-211C-GZ, Shanghaishiping

Laboratory Equipment, Shanghai, China) at 60 rpm. Each digestion flask featured two headspace interfaces: one end connected via rubber tubing to a gas collection bag (0.5 L, Dalianhaide Technology, Dalian, China) for venting and the other connected to a pressure gauge (GM522/range 0–100 kPa, Zhibiao Instrument, Shanghai, China) for measuring headspace pressure. The outlet tube was initially clamped to retain gas. After recording the pressure, the clamp was released to allow biogas to flow into the bag until the bottle pressure equilibrated with atmospheric pressure. Biogas composition was determined using gas chromatography (GC-2014-C, Shimadzu, Kyoto, Japan) equipped with a single thermal conductivity detector (TCD), with gas volume converted from pressure readings according to the following procedure: (i) the headspace pressure was recorded after each incubation period; (ii) the outlet clamp was released to vent biogas into the gas collection bag until the bottle pressure equilibrated with atmospheric pressure; (iii) the released gas volume at standard conditions was calculated using the ideal gas law (PV = nRT) based on the pressure differential, headspace volume (100 mL), and incubation temperature (37 ± 2 °C, 310 K); (iv) daily methane yield was obtained by multiplying the cumulative gas volume by the CH_4 fraction determined via GC. Gas sampling and analysis were conducted once daily throughout digestion.

Table 2. Experimental Design for Anaerobic Digestion of Long-chain Fatty Acids (LCFAs) with *Ruminococcus flavefaciens* Addition.

Group	LCFAs Types	Concentration of LCFAs (g/L)	Microbial Volume (*v*/*v*)
U	C18:1	10	0%
U + 0.1R	C18:1	10	0.1%
U + 0.5R	C18:1	10	0.5%
U + 1R	C18:1	10	1.0%
M	C18:0 + C18:1	5 + 5	0%
M + 0.1R	C18:0 + C18:1	5 + 5	0.1%
M + 0.5R	C18:0 + C18:1	5 + 5	0.5%
M + 1R	C18:0 + C18:1	5 + 5	1.0%
K	No LCFAs added	0	0%

Methane yield was normalised to the VS of the added LCFAs (i.e., LCFA mass, since pure stearic and oleic acids are effectively 100% volatile solids), not to inoculum VS or total reactor VS. Cumulative methane yield was calculated according to Equation (1):

$$Y_{CH_4} = \frac{V_{CH_4,group} - V_{CH_4,K}}{m_{VS,LCFA}} \quad (1)$$

where $Y(CH_4)$ is the cumulative methane yield (NmL CH_4 g^{-1} VS); V (CH_4, group) and V (CH_4, K) are the cumulative methane volumes (NmL, converted to normal conditions of 0 °C and 101.325 kPa) of the treatment group and of the inoculum blank K, respectively; and m (VS, LCFA) is the mass of LCFA volatile solids added per reactor, calculated as 10.00 g/L × 0.150 L = 1.50 g.

Digestive fluid samples (solid–liquid mixtures) were collected on days 0, 7, 14, and 21 for pH, TS, and VS determination. Following sampling, samples were centrifuged (TG-16G, Hunan Kecheng Instruments, Changsha, China) using a 12 × 5 mL angle rotor. The samples were centrifuged at 15,000 rpm for 3 min at 15 °C, and the supernatant was used for SCOD and AN analysis. Both metagenomic analyses and concentration analyses of *R. flavefaciens* were conducted on day 7. VFA analyses were conducted on days 7, 14, and 21. Four sampling time points (day 0, 7, 14 and 21) were predefined in this study, and metagenomic sequencing was performed on samples collected on day 7. As presented in

Section 3.1, the bioaugmented group achieved peak daily methane production on day 3. Sampling on day 7, the time point closest to the vigorous methanogenic phase, facilitates the elucidation of shifts in microbial community structure and functional genes under intense reaction conditions. This sampling time point was determined based on Gompertz model fitting; while day14 showed moderate biogas production, the lowest biogas production was observed on day 21. Samples were stored in a temperature-controlled freezer at −40 °C pending analysis (range at 0–−40 °C, Haier, Qingdao, China).

2.4. Analysis of Physical and Chemical Parameters

Headspace gases were collected using gas sampling bags and analysed by gas chromatography (GC-2014-C, Shimadzu, Kyoto, Japan). The instrument was equipped with a TCD and three packed columns (two P-N columns, 80/100 mesh, 3.2 mm inner diameter × 1.0 m length; one molecular sieve (MS)-13X column, 80/100 mesh, 3.2 mm inner diameter × 3.0 m length). Temperatures of the injection port, column oven, and detector were set to 150, 60, and 100 °C, respectively, with argon serving as the carrier gas. Gas samples were manually injected from the sampling bags using a syringe.

VFAs were analysed using a gas chromatograph equipped with an Rtx-Wax capillary column (30 m × 0.25 mm × 0.25 μm, Shimadzu, Kyoto, Japan) and a flame ionisation detector. pH was determined using a pH meter (PHSJ-4F with E-301-D electrode, Leici Product Marketing Centre, Shanghai, China). TS and VS were measured according to the American Public Health Association Standard Methods. SCOD and AN were analysed using commercial kits, with readings taken on a rapid digestion spectrophotometer (LH-3BN, Beijing Lianhua, Beijing, China).

2.5. Metagenomic Analysis

The cumulative methane yield curve was fitted using the Gompertz equation, day 7 was designated as the metagenomic sampling point because it was the closest scheduled sampling day to the maximum daily methane production phase (around day 3, Section 3.1) Metagenomic sequencing was performed on biological triplicate samples from each group (U_7 (unsaturated long-chain fatty acids treatment, samples collected on day 7), UR_7 (unsaturated long-chain fatty acids treatment supplemented with 1% *R. flavefaciens*, sampling on day 7), M_7 (mixed long-chain fatty acids treatment, samples collected on day 7), and MR_7 (mixed long-chain fatty acids treatment supplemented with 1% *R. flavefaciens*, sampling on day 7), n = 3 per group), yielding a total of 12 metagenomic datasets. All sequencing samples were derived from 12 completely independent anaerobic digesters with no sample pooling. A total of 39,701,472–46,434,382 raw read pairs were obtained for the 12 samples, with an average of 42,537,510 pairs per sample, corresponding to DNA extraction yields ranging from 0.420 μg to 1.178 μg. Based on the PE-150 sequencing strategy, the estimated sequencing depth ranged from 11.91 Gb to 13.93 Gb, with an average of 12.76 Gb per sample. For each group, digestive fluid samples were collected from three independent reactors on day 7 and individually subjected to DNA extraction and metagenomic sequencing. All downstream analyses of microbial community structure (PCoA, alpha-diversity indices) and functional gene abundance comparisons were conducted based on these replicate datasets. Raw reads were trimmed for 5′ and 3′ adapter sequences and filtered to remove short reads (<50 bp) and low-quality reads (average quality < 20) using fastp v0.23.0, and the remaining high-quality paired-end and single-end reads were assembled into contigs via MEGAHIT v1.1.2, with contigs longer than 300 bp retained. ORF prediction of contigs was performed using Prodigal (v2.6.3), and qualified genes (≥100 bp) were translated into amino acid sequences with EMBOSS 6.6.0. High-quality reads were mapped to the non-redundant gene set using SOAPaligner v2.21 at 95% identity

to calculate gene abundance. Gene abundance was normalised to reads per kilobase million (RPKM) to correct for variations in gene length and sequencing depth. Taxonomic and functional annotations were conducted by aligning amino acid sequences against the NR and KEGG databases using Diamond v0.8.35 (E-value < 1×10^{-5}), and the abundance of species and KEGG functional categories (KO, Pathway, EC, Module) was quantified. In addition, carbohydrate-active enzyme annotation was accomplished by hmmscan against the CAZy database (E-value < 1×10^{-5}), and the corresponding enzyme abundance was further calculated. Species classification and functional annotation of the metagenomic data were performed on the Majorbioe Cloud Platform.

2.6. Data Analysis

Cumulative methane yield $M(t)$ (NmL CH_4 g^{-1} VS) was fitted using a modified Gompertz model:

$$M(t) = P \cdot \exp\left\{-\exp\left[\frac{R_{\max}\,\mathrm{e}}{P}(\lambda - t) + 1\right]\right\} \quad (2)$$

Among these, P (NmL g^{-1} VS) denotes maximum methane potential, $R_{\max}$ (NmL g^{-1} VS·d^{-1}) denotes maximum methane generation rate, λ (d) represents the lag period, and bold italic e signifies the natural constant (2.71828). Significance tests were performed for all measured parameters across all sampling days (day 0, day 7, day 14, day 21), the day of maximum methane production (day 3), and the 24-day experimental endpoint. Independent intergroup comparisons were conducted separately at each individual time point. All experimental assays were performed in biological triplicates (n = 3). Pairwise group comparisons were carried out using two-tailed independent-samples Student's t-test with Welch's correction. Statistical analysis was conducted using IBM SPSS Statistics (version 28.0; IBM Corp., Armonk, NY, USA),with a significance level set at $p < 0.05$. No correction for multiple comparisons was applied to the pairwise tests of physicochemical parameters, as comparisons were conducted independently at each predefined sampling time point; the resulting p values should be interpreted accordingly. For the metagenomic comparisons, p values were adjusted using the Benjamini–Hochberg false discovery rate (FDR) procedure. All metagenomic statistical analyses were implemented on the Majorbio Cloud Platform. Principal coordinates analysis (PCoA) based on Bray–Curtis distances was used to visualise dissimilarities in microbial community structure across biological replicates, and PERMANOVA (permutational multivariate analysis of variance) was applied to test the significance of group differentiation. Wilcoxon rank-sum test was adopted to compare alpha-diversity indices (Chao1 and Simpson) and functional gene abundance between the control and bioaugmented groups. The Mantel test together with Pearson correlation analysis was employed to explore correlations between environmental physicochemical parameters and microbial community structure. Statistical significance was defined as $p < 0.05$ unless otherwise stated. All figures and tables were generated using OriginPro 2023 (OriginLab, Northampton, MA, USA) and Microsoft PowerPoint 2024 (Microsoft, Redmond, WA, USA).

3. Results and Discussion

3.1. Effect of R. flavefaciens on the Methane Production Performance of LCFAs

As shown in Figure 1, *R. flavefaciens* enhanced methane production from substrates containing unsaturated long-chain fatty acids (ULCFAs). The intensification effects positively correlated with dosages.

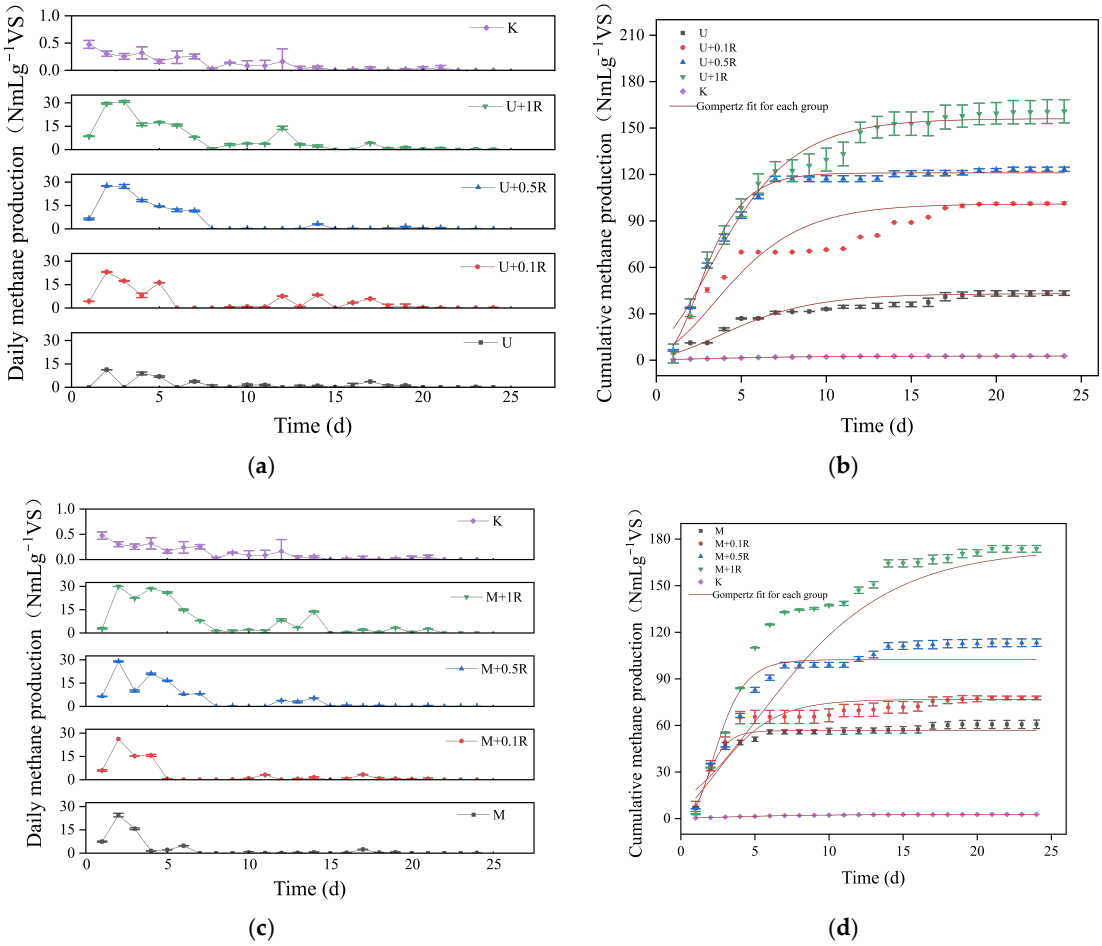


Figure 1. Methane production from anaerobic digestion of LCFAs at different *Ruminococcus flavefaciens* dosages: (**a**) daily methane yield from ULCFAs; (**b**) cumulative methane yield from ULCFAs and its Gompertz model fitting curve; (**c**) daily methane yield from MLCFAs; (**d**) cumulative methane yield from MLCFAs and its Gompertz model fitting curve. Error bars represent standard deviation, $n = 3$.

In experiments with *R. flavefaciens* additions of 0.1% (0.1R), 0.5% (0.5R), and 1% (1R) (v/v), 1% addition yielded optimal performance in cumulative methane production, maximum daily methane yield, and lag phase duration (Figure 1). In reactions containing only ULCFAs, cumulative methane yield in the control group U (ULCFAs) was 43.36 ± 1.47 NmL g^{-1} VS, indicating that the anaerobic digestion system was severely inhibited under the stress of ULCFAs. As *R. flavefaciens* dosage increased, methane production efficiency improved. The U + 1R (ULCFAs with the addition of 1% *R. flavefaciens*) group achieved a final methane yield of 160.82 ± 7.45 NmL g^{-1} VS, representing a 270.9% increase ($p = 0.001$) compared with the U group and was significantly higher than the low-dose groups (0.5R, 0.1R) ($p = 0.011$ and 0.005, respectively). In the mixed long-chain fatty acids (MLCFAs) reactions, the M + 1R (MLCFAs with the addition of 1% *R. flavefaciens*) group achieved a final methane yield of 173.68 ± 2.18 NmL g^{-1} VS, representing a significant 186.0% increase ($p < 0.001$), compared with the M (MLCFAs) group. The data indicate that the cumulative methane production of the M group is higher than that of the U group. This substantial relative increase reflects recovery from a severely inhibited baseline rather than enhancement of a normally functioning system, indicating that a 1% addition of *R. flavefaciens* effectively enhanced methane production potential in ULCFAs and MLCFAs reactions. Regarding maximum daily methane production, the U + 1R group reached 30.86 ± 0.59 NmL g^{-1} VS on day 3 (Figure 1a), being significantly higher than the U group (11.23 ± 0.05 NmL g^{-1} VS, $p = 0.003$). The M + 1R

group peaked at 29.99 ± 0.02 NmL g^{-1} VS, also being significantly higher than the M group (24.53 ± 1.14 NmL g^{-1} VS, $p = 0.028$). Regarding lag phase, the U group produced no gas on day 1, whereas the U + 1R group produced 8.56 ± 0.16 NmL g^{-1} VS on day 1. Cold storage may have transiently suppressed *R. flavefaciens* metabolic activity despite unchanged CFU concentration, which could have prolonged the lag phase. Nevertheless, the λ values of the bioaugmented groups (2.04 d for U + 1R and 1.92 d for M + 1R) were comparable to or even shorter than those of the controls (2.82 d for U and 2.66 d for M), and the U + 1R group produced gas on day 1, indicating that the inoculated cells rapidly resumed activity at 37 °C and that any cold-stress effect did not compromise the observed mitigation. As shown in Table 3, the Gompertz model also exhibits a similar trend. These findings indicate that *R. flavefaciens* addition shortened the lag phase and accelerated reaction onset, while extended lag phases are attributed to microbial acclimation or LCFA accumulation. The M group likely performed better than the U group because oleic acid appears to be the key inhibitory LCFA in oil-rich anaerobic digestion, whereas mixing distributes the LCFA load and can reduce oleic-acid-dominated inhibition [6,19]. This interpretation is consistent with the broader LCFA literature, which shows that inhibition in anaerobic digestion depends on the underlying mechanisms and operating conditions, so better performance in mixed LCFA systems is likely due to weaker unsaturated-fatty-acid stress rather than simply higher biodegradability [6]. Unlike saturated LCFAs, ULCFAs possess one or more cis-double bonds that introduce kinks into the hydrocarbon chain, enhancing membrane fluidity and permeability upon adsorption to microbial cell envelopes [20]. This structural feature enables oleate to integrate more readily into lipid bilayers, disrupting membrane integrity and directly impairing methanogenic activity—a mechanism that saturated stearic acid does not share to the same extent [21]. Consequently, the U experienced more severe membrane-level stress than the M, where the presence of stearic acid may have partially shielded methanogens from oleate-dominated membrane damage. *R. flavefaciens* possesses powerful organic matter degradation activity. High-dose addition accelerates polysaccharide degradation and promotes the production of VFA, particularly acetate. These fermentable intermediates provide substrates for downstream hydrogen-, acetate-, and methane-producing microorganisms, thereby enhancing the methane potential of the reactions [12,13]. The produced organic matter supplies available carbon sources, enhances microbial activity and mitigates LCFA inhibition [22]. *R. flavefaciens* may tolerate and alleviate LCFA toxicity via its unique cell-surface protein system even in lipid-rich substrates [11]. Moreover, cattle manure inoculum naturally harbours rumen-derived microorganisms. High-dose *R. flavefaciens* may synergise with indigenous communities (such as other *Ruminococcus* spp. and *Fibrobacter*) to enhance activation and acidification rates. Rumen microbiota exhibits adaptive responses to LCFAs, indirectly promoting β-oxidizing bacteria (such as *Syntrophomonas* spp.) [23].

It should be noted that although the relative increase in methane yield upon *R. flavefaciens* addition is substantial (up to 270.9%), the absolute cumulative production (160.82–173.68 NmL g^{-1} VS) is still modest relative to the theoretical methane potential. This limited absolute recovery may be attributed to the following factors. First, the applied LCFA loading of 10.00 g/L markedly exceeds the microbial tolerance threshold, potentially causing severe adsorption of LCFAs onto inoculum biomass and reducing substrate bioavailability. Second, the use of pure LCFAs as sole carbon sources lacks readily fermentable co-substrates (e.g., proteins, carbohydrates) that typically support robust methanogenic activity in complex wastes. Third, the low absolute yield at the 24-day endpoint suggests that the severe physicochemical inhibition established by the supra-threshold LCFA loading may have prevented complete β-oxidation.

Table 3. Gompertz Model-Fitted Data Under the Addition of *Ruminococcus flavefaciens* for LCFA Anaerobic Digestion.

Groups	P (NmL g^{-1} VS) (95% CI)	R_{max} (NmL g^{-1} VS·d^{-1}) (95% CI)	λ (d) (95% CI)	R^2	RMSE
U	43.38 (40.21, 46.55)	5.92 (5.24, 6.60)	2.82 (2.43, 3.21)	0.97	1.47
U + 0.1R	99.42 (94.83, 104.01)	7.94 (7.19, 8.69)	3.40 (2.98, 3.82)	0.98	1.84
U + 0.5R	121.81 (117.33, 126.29)	13.72 (12.58, 14.86)	2.28 (1.95, 2.61)	0.98	2.08
U + 1R	160.68 (155.64, 165.72)	16.34 (14.97, 17.71)	2.04 (1.71, 2.37)	0.98	2.68
M	59.20 (55.48, 62.92)	6.83 (6.07, 7.59)	2.66 (2.29, 3.03)	0.97	1.62
M + 0.1R	77.83 (73.98, 81.68)	8.74 (7.94, 9.54)	3.14 (2.73, 3.55)	0.98	1.95
M + 0.5R	112.11 (107.36, 116.86)	14.41 (13.21, 15.61)	2.16 (1.82, 2.50)	0.98	2.19
M + 1R	173.38 (168.25, 178.51)	17.18 (15.78, 18.58)	1.92 (1.58, 2.26)	0.98	2.81
K	2.67 (1.87, 3.47)	0.38 (0.22, 0.54)	4.22 (3.30, 5.14)	0.94	0.39

In summary, high-dose *R. flavefaciens* may mitigate ULCFA inhibition and enhance methane production via synergistic activation, acidification, tolerance to LCFA toxicity through its unique cell-surface protein system, and cooperation with *Syntrophomonas*. No additional control group containing only inoculum and 1% (*v*/*v*) *R. flavefaciens* without LCFA substrates was established in this study. *R. flavefaciens* is a non-methanogenic cellulolytic bacterium (phylum Firmicutes) that lacks key methanogenic enzymes (e.g., methyl-coenzyme M reductase) and produces only H_2, CO_2, and acetate as metabolic end products [14,23]; it therefore cannot produce methane directly. However, the H_2 and acetate released by the inoculated strain may be converted to methane by the indigenous methanogenic community, and thus part of the observed methane increase could originate indirectly from the fermentation products of *R. flavefaciens* rather than exclusively from enhanced LCFA conversion. This limitation should be acknowledged, and an *R. flavefaciens*-only control is required in future work to quantitatively separate these contributions.

3.2. Effects of R. flavefaciens on Physico-Chemical Parameters During the Digestion of Different Substrates

The impact of *R. flavefaciens* bioaugmentation on anaerobic digestion stability under substrates containing ULCFAs was evaluated by comparing changes in VS removal rates, SCOD conversion rates, and AN concentration (Figure 2). AN was analysed to evaluate the risk of ammonia inhibition throughout the experiment. The results indicated that the role of *R. flavefaciens* in promoting substrate degradation was significantly correlated with its addition rate, enhancing degradation efficiencies while also maintaining reaction stability.

VS removal rate characterizes the capacity of a reaction to degrade soluble organic matter (Figure 2a). Statistical analysis revealed that *R. flavefaciens* addition enhanced overall substrate degradation efficiency, with VS removal rates increasing alongside elevated dosages. In reactions containing only ULCFAs, VS removal rate in the U + 0.1R group was 24.84 ± 1.78%, exhibiting no significant difference compared with that of the control group U (23.80 ± 0.97%) ($p > 0.05$). When addition rate increased to 0.5% and 1%, removal rates rose to 27.63 ± 0.60% and 29.79 ± 1.05%, respectively; both were significantly higher than that of the control group ($p < 0.05$). In the MLCFAs reactions, VS removal rate in the M + 0.1R group was 29.44 ± 1.34%, significantly higher than that in the M control group (24.97 ± 1.92%) ($p = 0.03$). With increasing addition dosages, VS removal rates further increased to 33.85 ± 1.52% (M + 0.5R group) and 35.00 ± 1.35% (M + 1R group); both were significantly higher than those of the control group ($p < 0.05$). These results indicate that *R. flavefaciens* addition enhanced the overall removal of solid organic matter during anaerobic digestion of ULCFAs-containing substrates, with removal rates exhibiting an upward trend as *R. flavefaciens* dosages increased.

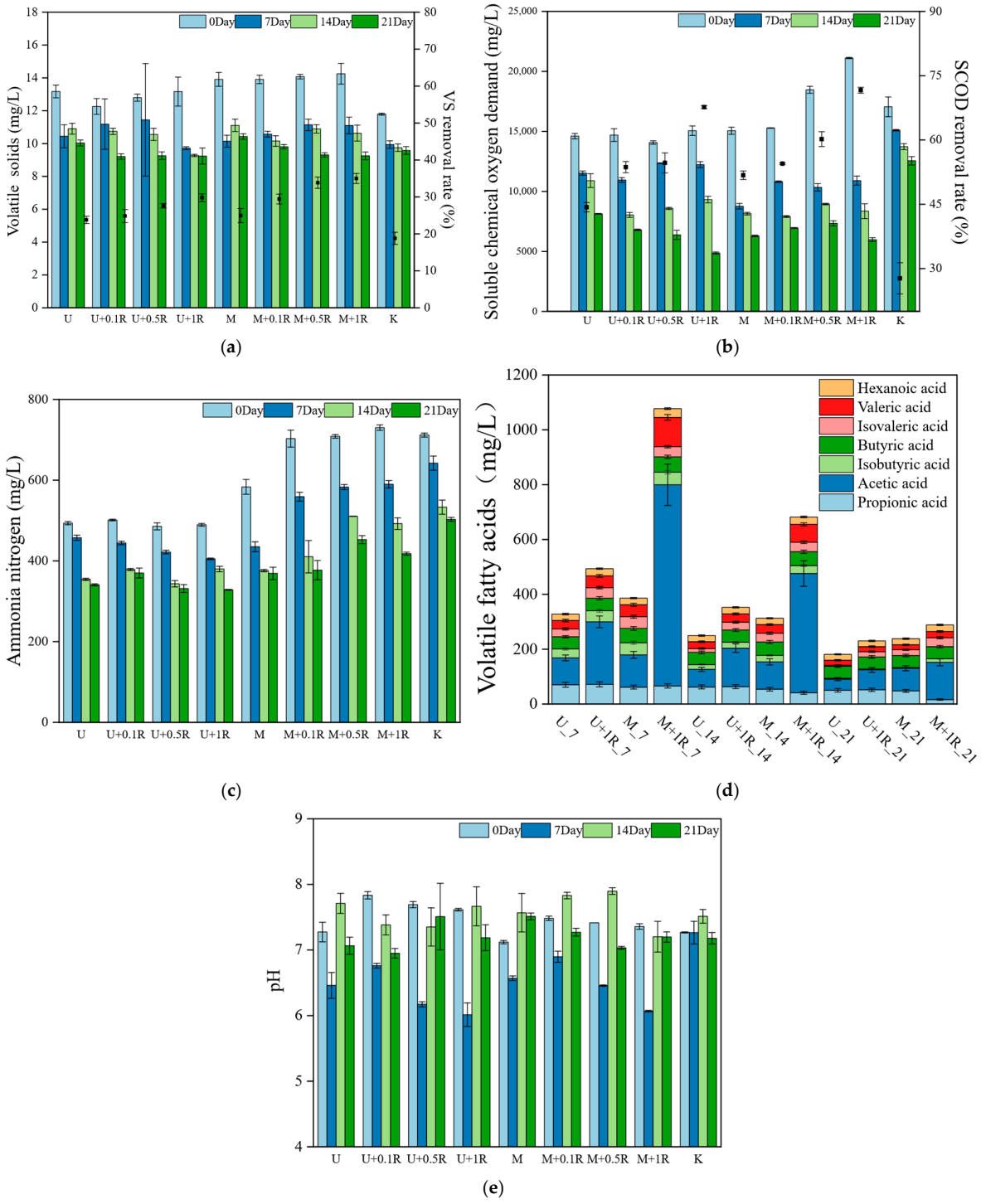


Figure 2. Changes in physicochemical indicators of anaerobic digestion with varying doses of *Ruminococcus flavefaciens*: (**a**) VS concentration, and black square markers represent the VS removal rate (%) (**b**) variations in the aqueous dissolved SCOD concentration and black square markers represent the SCOD removal rate (%). Note that SCOD removal reflects only the dissolved aqueous fraction plus physical adsorption of LCFAs/intermediates onto biomass and cannot be interpreted as whole-system Total COD (TCOD) removal. (**c**) variations in AN concentration (**d**) comparison of VFA concentrations (**e**) comparison of pH variations.

SCOD removal efficiency serves as an indicator for the conversion of dissolved organic matter during anaerobic digestion. As shown in Figure 2b, in reactions containing only ULCFAs, the control group U exhibited a SCOD removal rate of 44.32 ± 1.08%. The

U + 1R group demonstrated a significantly increased SCOD removal rate of 67.67 ± 0.32% ($p < 0.01$). In the MLCFAs reactions, the M + 1R group exhibited the highest SCOD removal rate (71.61 ± 0.68%), significantly surpassing the control group M (51.77 ± 0.99%, $p < 0.01$) and the M + 0.5R group (60.20 ± 1.74%, $p = 0.01$). It is worth noting that these SCOD removal discrepancies are affected by the divergent initial SCOD values at Day 0 among treatments. Initial SCOD on day 0 ranged from 15,000 to 20,000 mg/L among all treatments. The variations were closely related to LCFA supplementation: exogenous LCFAs could lower the initial SCOD. Notably, Group K exhibited higher initial SCOD at day 0 compared with all LCFA-amended treatments. This difference stems from the physical property of LCFAs: these substances possess extremely low solubility in neutral water and form free-floating oil droplets upon addition. The oily phase is separated and removed via centrifugation before SCOD quantification, so the detected SCOD only reflects dissolved organics in the aqueous phase rather than the overall total organic load of the system. It should be noted that the observed SCOD removal may partially reflect the adsorption of LCFAs and their intermediates onto biomass, as LCFAs are known to readily adsorb onto anaerobic sludge [24]. This adsorption effect may overestimate the actual biodegradation efficiency. Therefore, the SCOD removal rates reported in this study reflect the conversion of the aqueous dissolved organic fraction together with physical adsorption of LCFAs and their intermediates onto biomass, and should not be interpreted as whole-system Total COD (TCOD) removbiomass andenic performance should be assessed primarily based on cumulative methane yield. Nevertheless, the concomitant increase in cumulative methane production suggests that microbial degradation was also enhanced. In summary, 1% (v/v) dosages of *R. flavefaciens* significantly enhanced the degradation efficiency of dissolved organic matter during anaerobic digestion of LCFAs. *R. flavefaciens* addition did not result in abnormal AN accumulation (Figure 2c). In reactions containing only ULCFAs, although the U + 1R group exhibited the highest substrate degradation level, its endpoint AN concentration was 328.4 ± 0.96 mg/L, exhibiting no significant difference compared with that of the control group U (340.7 ± 2.61 mg/L) ($p > 0.05$). In the MLCFAs reactions, the M + 1R group exhibited a peak AN concentration exceeding that of the control group on day 7 ($p = 0.01$), consistent with its higher VS removal rate. By the final sampling point of the reactions (day 21), AN concentration had declined to 417.8 ± 3.91 mg/L, exhibiting no significant difference compared with that of the control group M (368.9 ± 15.54 mg/L) ($p > 0.05$). AN released at these concentrations decreased due to pH and assimilation by microbial growth, thereby preventing inhibition. Overall, AN concentrations in all groups remained below the ammonia inhibition threshold (<750 mg/L) [25], with reactions maintaining stable metabolism under *R. flavefaciens* addition at all concentrations.

The composition of VFAs and pH changes are shown in Figure 2d,e. *R. flavefaciens* addition promoted acetate production in both reactions containing only ULCFAs and MLCFAs. During the LCFA conversion and acidification (day 7), LCFAs were converted into VFAs. Total VFA concentrations in M + 1R and U + 1R were 1077.26 and 493.57 mg/L, respectively; both were higher than those of their respective control groups. On day 7, acetic acid concentrations in the M + 1R and U + 1R reactions were 733.79 (68.12% of total VFA) and 228.01 mg/L (46.20% of total VFA), respectively. Propionic acid, which inhibits anaerobic digestion, remained at low levels (<72 mg/L). Rapid acetate production temporarily lowered the pH of anaerobic digestion to 6.01 ± 0.18–6.07 ± 0.12 in the early phase. A slight increase in acidification was observed at high dosages of *R. flavefaciens*, which likely facilitated the conversion of SCOD into acetate. During the same period, U and M showed significantly lower levels compared with the U + 1R and M + 1R groups ($p < 0.05$). By day 14, total VFA concentrations in M + 1R and U + 1R decreased to approximately 682.24 and 352.50 mg/L, respectively, yet remained significantly higher than those in the

control groups (M: 312.80 mg/L; U: 249.68 mg/L). Acetic acid continued to dominate the VFA profile in the bioaugmented groups, accounting for approximately 63.80% and 39.75% of total VFAs in M + 1R and U + 1R, respectively, while propionic acid remained below 70 mg/L across all groups. These intermediate measurements suggest that methanogenic consumption of acetate had commenced while acidification remained active, illustrating the metabolic transition between the two phases. Upon entering methanogenesis, acetate was continuously consumed [26]. By day 21, VFA degradation rates in the M + 1R and U + 1R groups reached 73.21% and 53.36%, respectively. As acetate was consumed, pH gradually rebounded, stabilising at approximately 7.20 ± 0.20 by the final sampling point (day 21), exhibiting no significant difference from that of the control group ($p > 0.05$). In summary, *R. flavefaciens* addition may have effectively promoted the conversion of intermediate products to methane while also ensuring stable reaction progression by enhancing acetate supply and preventing propionic acid accumulation [27].

3.3. Effects of *R. flavefaciens* on Microbial Populations and Structure

Concentration analysis of *R. flavefaciens* confirmed its survival throughout anaerobic digestion. At day 0, the bioaugmented groups (U + 1R and M + 1R) exhibited initial abundances of 1.0×10^6 CFU/mL, consistent with the initial cell density estimated from the 1% (*v*/*v*) inoculation of the 10^8 CFU/mL stock (Section 2.3). By day 7, *R. flavefaciens* remained at high levels, with abundances of 4.2×10^7 CFU/mL in the U + 1R group and 7.5×10^7 CFU/mL in the M + 1R group. Conversely, no target colonies were detected in the non-bioaugmented controls (U and M) at day 7 ($<1.0 \times 10^3$ CFU/mL), confirming that the detected signal originated exclusively from the inoculated strain rather than indigenous *Ruminococcus* species present in the cattle manure inoculum. These results demonstrate that exogenous *R. flavefaciens* successfully survived and maintained considerable cultivable populations under LCFA inhibition.

On day 7, samples from the U_7, UR_7, M_7 and MR_7 groups were selected for metagenomic analysis. A total of 1,084,085,272 raw reads were generated. After quality control and removal of low-quality sequences and adapters, 1,076,518,680 clean reads were obtained and used for subsequent bioinformatic analyses. Analysis of coverage, Chao1, and Simpson indices (Figure 3a–c) revealed that *R. flavefaciens* did not significantly alter microbial richness or evenness during anaerobic digestion under different substrate conditions. Specifically, the coverage index approached 1.0, indicating sufficient sequencing depth to cover most taxa and ensuring representativeness of the analysis. The Chao1 index indicated that differences in species richness were marginally significant ($p = 0.065$). The Simpson index exhibited minimal variation in reactions containing only ULCFAs, whereas the MR_7 group exhibited an increase in the Simpson index in the MLCFAs reactions, although this increase was not significant ($p = 0.086$). These results indicate that *R. flavefaciens* addition may enhance microbial community evenness in the MLCFAs reactions, whereas it exerts a reduced effect on microbial community evenness in the ULCFA reactions. Principal coordinates analysis (Figure 3d) revealed that *R. flavefaciens* addition significantly influenced microbial community structure ($p = 0.002$), with microbial abundance closely correlating to *R. flavefaciens* dosages.

To elucidate the microbial mechanisms enhancing methanogenic performance following *R. flavefaciens* addition, bacterial (Figure 3e) and archaeal (Figure 3f) community compositions at the genus level across reactions were analysed, with results expressed as relative abundances (%). As shown in Figure 3, *R. flavefaciens* addition enriched key functional genera associated with LCFA degradation. In reactions containing only ULCFAs, the relative abundance of *Xiashengella* (phylum: Bacteroidota) increased from 4.64% in the control group U_7 to 5.48% in the UR_7 group. This genus can ferment to produce

succinic acid and participates in complex organic matter degradation [28], suggesting that the addition of *R. flavefaciens* may promote related utilisation or fermentation functions. The relative abundance of *Bacteroides* (phylum: Bacteroidota) also increased from 2.67% to 3.40%. *Bacteroides* can convert substrates into VFAs, producing acetate and succinate; these intermediates can further transform into propionate, thereby supplying electron acceptors and carbon sources for anaerobic fermentation [29]. Consequently, *R. flavefaciens* addition increased the abundance of Bacteroidota phylum members during ULCFA reactions, potentially enhancing acidification product supply and boosting methane yield. This enrichment was more pronounced in the MLCFAs reactions: *Xiashengella* abundance rose to 9.96% in the MR_7 group, exceeding the 6.22% abundance observed in the M_7 group. Concurrently, the abundance of the cellulolytic bacterium *Ruminiclostridium* (phylum: Firmicutes) increased from 2.20% to 3.18% in the MR_7 group. *Ruminiclostridium* breaks down organic substrates to yield VFAs, mainly acetate [25], offering a possible microbiological basis for the enhanced VS and SCOD removal rates following *R. flavefaciens* bioaugmentation. Notably, *R. flavefaciens* addition was associated with a modest increase in the syntrophic β-oxidizing bacterium *Syntrophomonas* (phylum: Firmicutes). This genus degrades LCFAs via β-oxidation, producing acetate, H_2, and CO_2 [30]. In the UR_7 and MR_7 groups, *Syntrophomonas* abundance increased to 1.08% (control: 0.88%) and 1.34% (control: 1.10%), respectively, which may contribute to acetate supply for downstream methanogenesis.

Methanosarcina attained a dominant position within the archaeal community structure during the reaction (Figure 3f). In reactions containing only ULCFAs, the relative abundance of *Methanosarcina* increased from 66.43% in the U_7 group to 69.63% in the UR_7 group following its addition, whereas in the MLCFAs reactions, it increased from 67.42% in the M_7 group to 75.20% in the MR_7 group. *Methanosarcina* possesses acetate utilisation capability and strong environmental tolerance [31]. Its increased abundance aligns with rapid acetate consumption and pH elevation observed in the VFA analysis (Section 3.2). Concurrently, hydrogenotrophic archaea, potentially involved in syntrophic β-oxidation with *Syntrophomonas*, were retained in all groups: *Methanobacterium* (UR_7 group: 5.96%) and *Methanoculleus* (MR_7 group: 3.18%) [32]. The observed increases in *Syntrophomonas* and *Methanosarcina* abundances were relatively modest. However, under severe LCFA inhibition (10.00 g/L), maintaining these rate-limiting functional guilds is critical; even slight enrichment can strongly alter metabolism [33]. Because taxonomic abundances were calculated as RPKM-normalized relative values, these modest shifts should be interpreted cautiously; they may reflect either genuine enrichment or relative changes driven by declines in other taxa. Their biological relevance is therefore inferred primarily from their coherence with elevated β-oxidation and methanogenesis gene abundances (Section 3.5) and the concomitant improvements in methane production and acetate turnover, rather than from their magnitude alone. The community structure is consistent with a putative syntrophic metabolic association centred on *Syntrophomonas-Methanobacterium-Methanosarcina,* which is potentially formed within the *R. flavefaciens*–supplemented system. This proposed arrangement may facilitate the timely consumption of acetate and hydrogen, potentially supporting efficient and stable progression of methanogenesis [30].

While specific genera are discussed above in relation to enhanced performance, anaerobic microbiomes typically exhibit substantial functional redundancy, and equivalent metabolic roles may be performed by multiple uncharacterized taxa [34]. The observed shifts in community structure should therefore be interpreted as correlating with, rather than exclusively driving, improved functional performance.

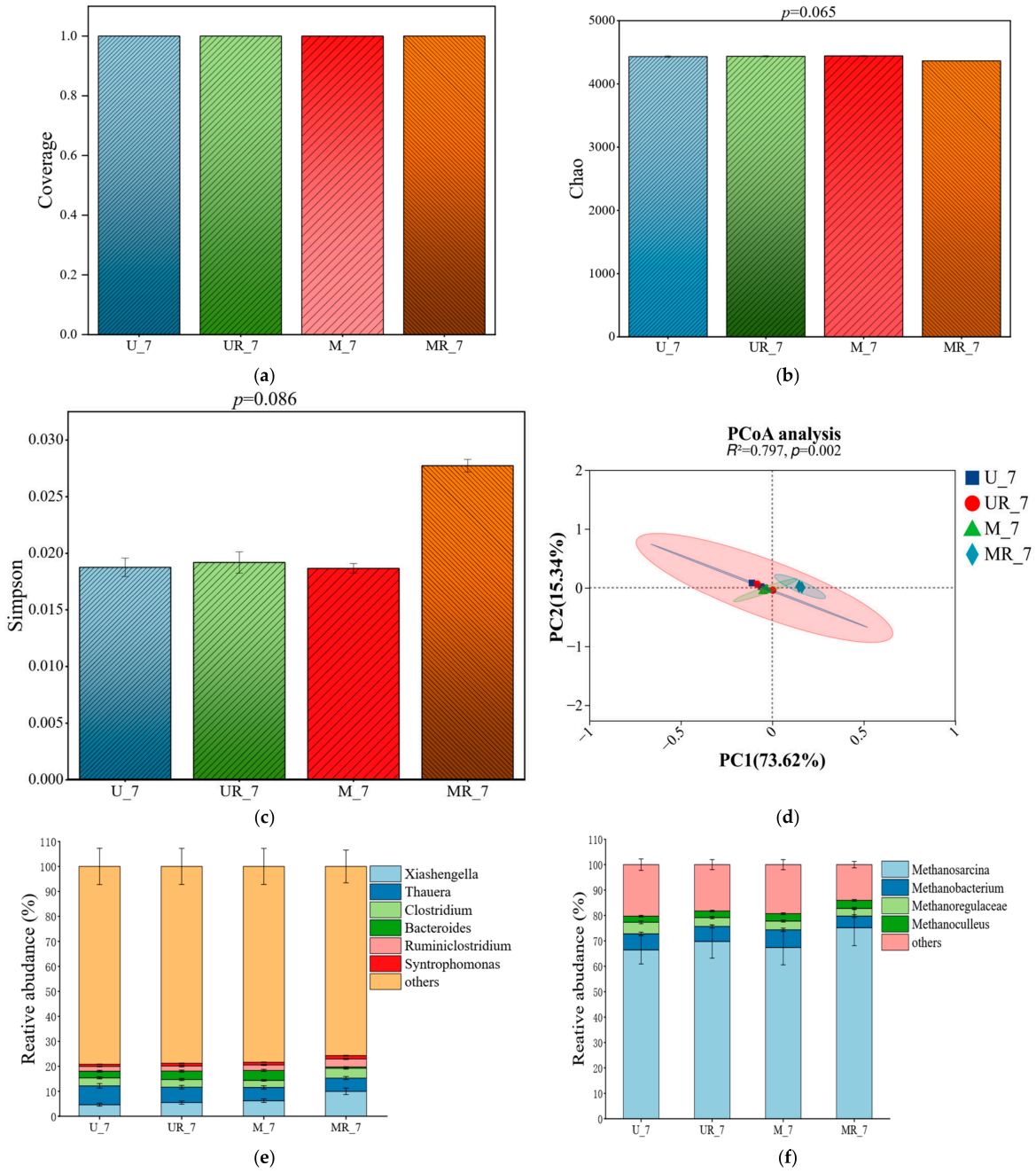


Figure 3. Microbe-related changes in ULCFAs and MLCFAs reactions following *Ruminococcus flavefaciens* addition: (**a**) coverage index analysis (**b**) Chao1 index species richness assessment (**c**) Simpson index community evenness analysis (**d**) principal coordinates analysis (PCoA) based on Bray–Curtis distances. Each point represents one biological replicate (n = 3 per group); shaded ellipses represent 95% confidence intervals; dashed lines indicate the zero reference axes (no statistical meaning); R^2 and p values were obtained by PERMANOVA (Adonis, 999 permutations), where R^2 represents the proportion of community variation explained by grouping (**e**) bacterial community structure changes; (**f**) archaeal community structure changes.

3.4. Correlation Analysis Between Physico-Chemical Parameters and Changes in Microbial Community Structure

Combined analysis of the Mantel test and Pearson correlation heatmap (Figure 4) revealed associations between anaerobic digestion performance, changes in microbial community structure, and environmental physicochemical parameters. The results indicate that cumulative methane production and maximum daily methane production were

significantly positively correlated with overall microbial community structure. The bioaugmentation achieved by adding *R. flavefaciens* was associated with adjustments in microbial community structure, showing a close association with increases in methane production capacity under LCFA conditions. The dominant methanogenic archaeon *Methanosarcina* exhibited a positive correlation with methane production and VFA concentrations, consistent with a potential involvement in acetate metabolism and suggesting robust adaptability under high acetate loading conditions. Concurrently, hydrolytic bacterial genera *Xiashengella*, *Ruminiclostridium*, and *Fibrobacter* exhibited significant positive correlations with VS removal rates, consistent with higher abundances of hydrolytic populations upon *R. flavefaciens* addition, which could partly explain enhanced VS removal. The Pearson correlation matrix revealed positive relationships between upstream hydrolytic bacteria, such as *Xiashengella* and *Ruminiclostridium*, and the downstream methanogenic archaeon *Methanosarcina*. This finding suggests that the bioaugmented anaerobic digestion of LCFAs involving *R. flavefaciens* may potentially form a stable, tightly coupled cascade of hydrolysis, acidification, and acetate-type methanogenesis. This putative mechanism may facilitate the rapid conversion of volatile intermediate products such as VFAs, potentially mitigating LCFA accumulation and inhibition and supporting stable and sustained gas production [35].

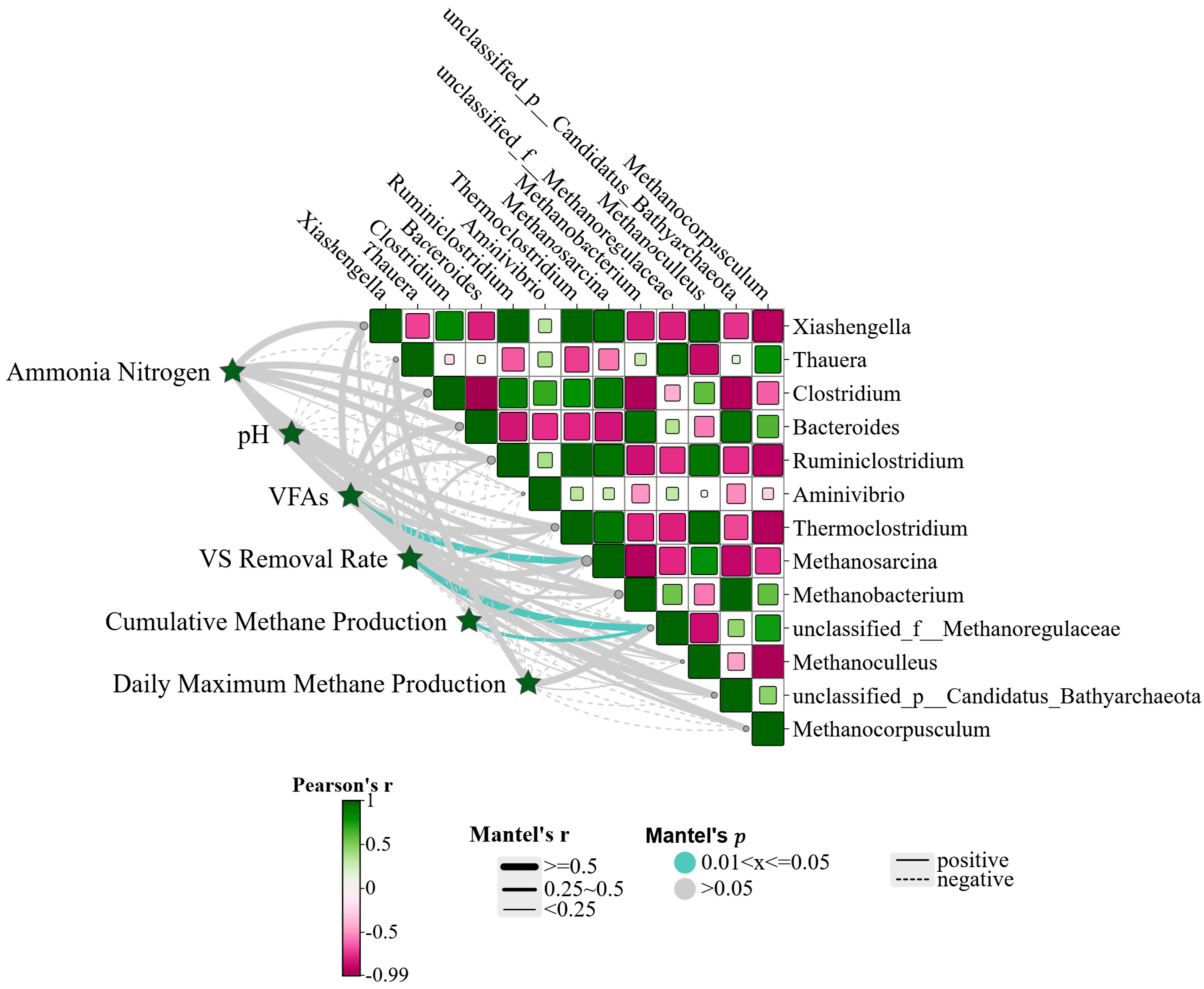


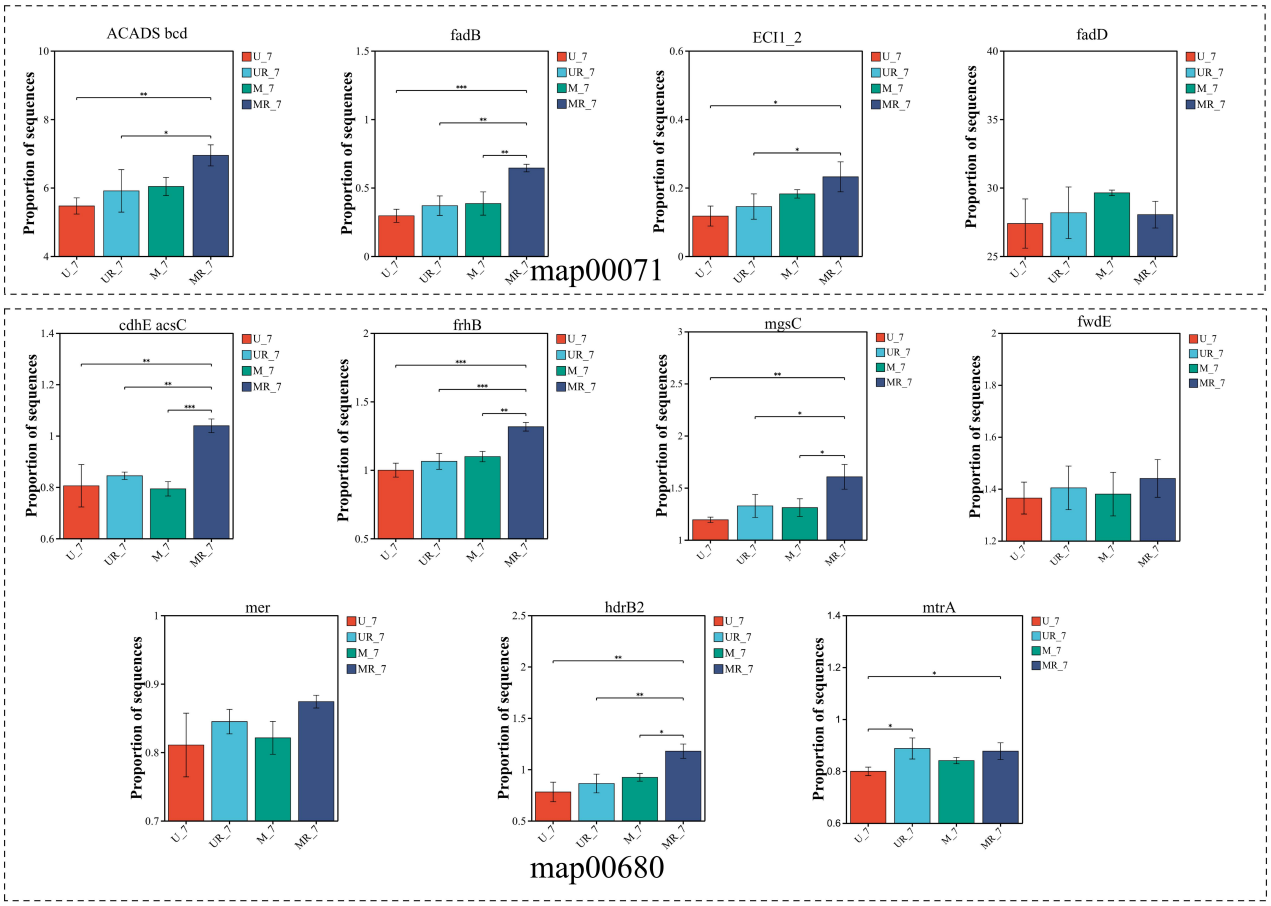
Figure 4. Correlation analysis between environmental factors and changes in microbial community structure following *Ruminococcus flavefaciens* addition. Stars indicate significant Mantel test results ($p < 0.05$).

3.5. Effects of R. flavefaciens on Anaerobic Digestion Pathways for LCFAs

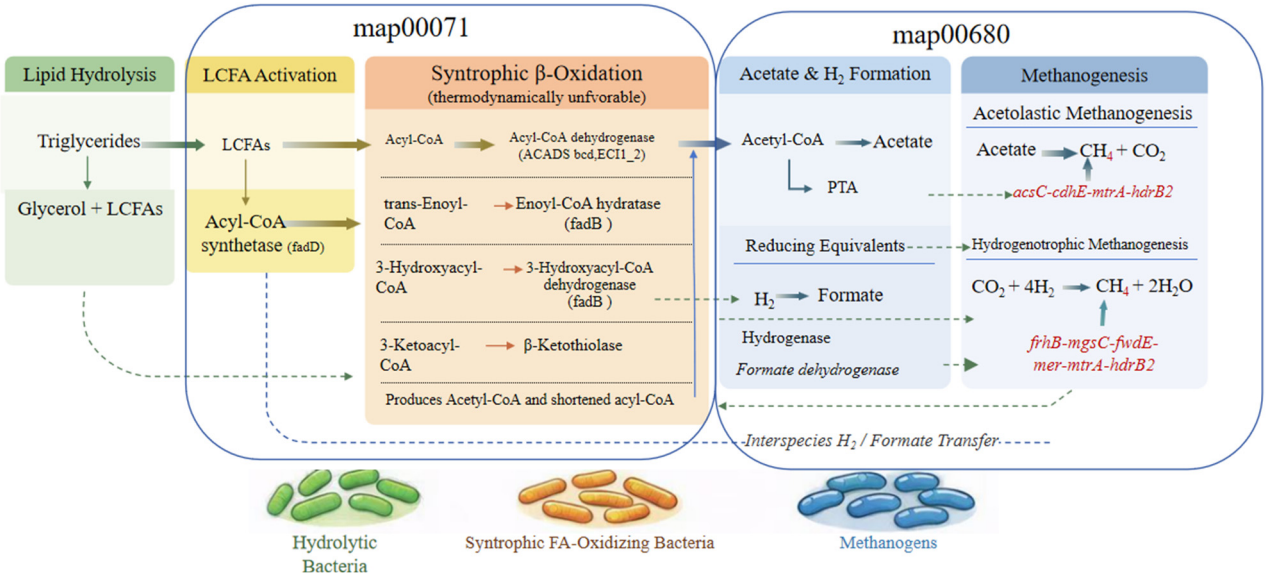
A comprehensive quantitative analysis of LCFA metabolism-related functional genes revealed that the addition of *R. flavefaciens* increased the relative abundance of key functional genes for the conversion of LCFA substrates to final methanogenic products. This finding suggests potential for mitigating LCFA conversion bottlenecks.

During β-oxidation, the key rate-limiting step in high-lipid anaerobic digestion [6], the MR_7 and UR_7 groups exhibited significant enrichment of associated functional genes (Figure 5a). Following *R. flavefaciens* addition, the relative abundance of the key enzyme–encoding genes Acyl-CoA Dehydrogenases/Butyryl-CoA Dehydrogenase (*ACADs/bcd*, K00249/K00248) increased significantly ($p < 0.05$). Concurrently, Enoyl-CoA hydratase (*fadB*, K01825), a multifunctional enzyme possessing acyl-CoA hydratase and 3-hydroxyacyl-CoA dehydrogenase activities, and the core enzyme Enoyl-CoA Δ^3-Δ^2-isomerase 1 (ECI1_2, EC 5.3.3.8), which specifically catalyses ULCFA isomerisation, also exhibited an increasing trend. Combined with enrichment of the LCFA-activating gene Fatty acyl-CoA synthetase (*fadD*, K01897), this finding suggests that *R. flavefaciens* addition may be associated with potential for ULCFA activation and β-oxidation. The increase in gene abundance across the entire pathway aligns with elevated acetate proportion and enhanced methane production observed in the *R. flavefaciens*-supplemented group, suggesting a potential for converting LCFA into acetate (Figure 5b) [36].

Analysis of methanogenic functional genes indicated that supplementation with *R. flavefaciens* could raise the relative abundance of methane-metabolising genes. In the ULCFA-MLCFA reactions (UR_7 and MR_7 groups), key genes ensuring stable progression of the acetate-dependent methanogenesis pathway, such as CO dehydrogenase/acetyl-CoA synthase complex subunit gamma (*cdhE*, K00197), exhibited significantly higher relative abundance than those in the control group ($p < 0.001$), consistent with the enrichment trend of the dominant methanogenic archaeon *Methanosarcina*. This observation suggests potential for improved acetate-cleavage capacity. Concurrently, hydrogen-dependent methanogenesis-related genes, such as F420-reducing hydrogenase subunit B (*frhB*, K00441) and methylamine—glutamate N-methyltransferase subunit C (*mgsC*, K22083), exhibited increased abundance, which may indicate higher abundance of genes linked to interspecies hydrogen or electron transfer to support LCFA oxidation and maintain low hydrogen partial pressure [37]. Additionally, formylmethanofuran dehydrogenase subunit E (*fwdE*, K11261), which catalyses the initial reductive step of hydrogenotrophic methanogenesis, and 5,10-methylenetetrahydromethanopterin reductase (*mer*, K00320), involved in methyl transfer within the hydrogenotrophic pathway, both exhibited elevated relative abundances in the bioaugmented groups (UR_7 and MR_7) compared with their respective controls. Moreover, Heterodisulfide reductase subunit B2 (hdrB2, K03389) and Methyltransferase subunit A (*mtrA*, K00577) genes, which are associated with terminal energy conversion, also exhibited significant enrichment in the bioaugmented group, indicating potential for improvements in the methanogenic electron transport system. Conversely, functional gene abundances exhibited reduced variation during ULCFA reactions and did not follow the upward trend observed in MLCFA reactions. This finding suggests that *R. flavefaciens* may be susceptible to ULCFA inhibition, resulting in limited increases in relevant gene abundances during metabolic processes. It should be noted that gene abundance alone cannot confirm actual pathway activation; nevertheless, these genomic signatures reflect the reservoir of methanogenesis-related genes within the community. A larger reservoir of such genes provides a prerequisite for methanogenic populations to cope with LCFA-induced inhibition and sustain methane production when inhibitory pressure is alleviated. The extent to which these genomic signatures translate into functional pathway activation warrants further investigation.



(**a**)



(**b**)

Figure 5. Addition of *Ruminococcus flavefaciens* to ULCFAs and MLCFAs reactions: (**a**) relative abundance of functional genes encoding key enzymes in LCFA anaerobic degradation (* $p < 0.05$, ** $p < 0.01$, *** $p < 0.001$); (**b**) key metabolic pathways for LCFAs. Solid arrows indicate metabolic conversion steps; dashed arrows indicate metabolic coupling among functional guilds; colored blocks indicate functional modules; red gene symbols indicate genes involved in methanogenesis; black gene symbols indicate constituent enzymes of the LCFA degradation pathway.

3.6. Effects of *R. flavefaciens* on CAZymes

LCFAs exert inhibitory effects by physically adsorbing onto and disrupting microbial cell membranes. Elevated abundances of CAZyme-encoded glycosyltransferases (GTs), which participate in cell-membrane and cell-wall biosynthesis, indirectly suggest microbial cell-envelope remodelling to counteract LCFA toxicity [38], ultimately with potential for improving system gas production performance and stability.

To investigate the impact of *R. flavefaciens* addition on microbial structural biosynthesis and stress tolerance during anaerobic digestion of LCFAs, changes in CAZymes functionality were analysed via metagenomics, as depicted in Figure 6. The Wilcoxon rank-sum test revealed that in the MLCFAs reactions (Figure 6a), *R. flavefaciens* addition increased members of the GT family, particularly GT2 and GT4, in MR_7 relative to M_7. GT enzymes participate in polysaccharide backbone synthesis and extracellular polysaccharide formation, according to previous reports, which may potentially support biofilm-related processes. If such structures were formed, they could shorten mass transfer distances between microbial communities, facilitating metabolite and electron exchange [39–41]. Accordingly, *R. flavefaciens* bioaugmentation may enhance EPS synthesis potential, thereby promoting the generation of functional microbial communities to maintain metabolic activity and system stability.

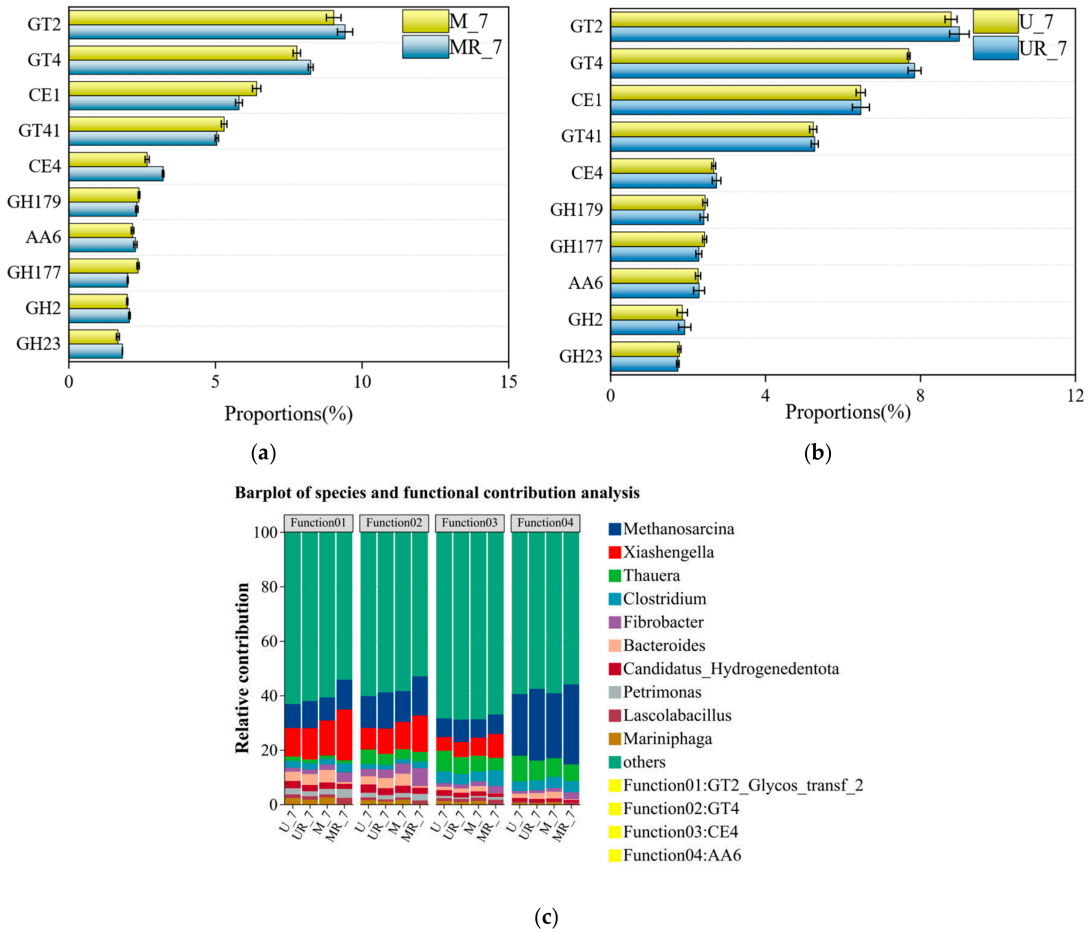


Figure 6. Differential analysis of carbohydrate-active enzymes (CAZymes) in ULCFAs and MLCFAs reactions following *Ruminococcus flavefaciens* addition: (**a**) M group (**b**) U group (**c**) species contribution analysis of carbohydrate-active enzymes.

Furthermore, Carbohydrate Esterase family 4 (CE4), including chitin deacetylase, exhibited an upward trend following *R. flavefaciens* addition. It modifies acetyl groups of

microbial cell walls and extracellular polymeric components to reduce steric hindrance, contributing to cell-envelope remodelling and biofilm assembly [42]. These functional alterations suggest that *R. flavefaciens* bioaugmentation may strengthen microbial cell-envelope biosynthesis and biofilm-forming potential. Concurrently, AA6 (1,4-benzoquinone reductase) exhibited an increasing trend following *R. flavefaciens* bioaugmentation. This enzyme participates in the quinone/hydroquinone cycle, reducing the benzoquinone intermediate. This process helps mitigate the potential toxicity of phenolic and quinone active intermediates and oxidative stress. The enrichment of AA6 suggests that *R. flavefaciens* may indirectly safeguard microbial physiological functions by enhancing detoxification functions, potentially alleviating oxidative stress within the microbial community.

Following the addition of *R. flavefaciens* to reactions containing only ULCFAs, certain CAZymes, such as GT2, GT4, CE4, and AA6, exhibited an increasing trend (Figure 6b), although the overall functional enhancement was less pronounced than that in MLCFA reactions. This discrepancy indicates that the potential of *R. flavefaciens* to boost microbial structural biosynthesis and stress-resistance capacity is constrained by ULCFAs, which exert a more detrimental effect on high-fat anaerobic digestion than saturated LCFAs.

Species contribution analysis (Figure 6c) further elucidated the correspondence between functional groups and species. Following *R. flavefaciens* addition, contribution ratios of bacterial genera *Xiashengella* and *Thauera* within the GT (cell-envelope and EPS synthesis) and CE (cell-wall deacetylation for structural remodelling) functional groups increased markedly. These genera may facilitate microbial cell-envelope remodelling and biofilm assembly and support methanogenic archaea. The archaeon *Methanosarcina* also exhibited high contribution ratios across GT2, GT4, CE4, and AA6 functional categories. Beyond methanogenesis, it may participate in cell-envelope biosynthesis, biofilm formation and quinone-based detoxification, potentially improving carbon-metabolism coordination and redox balance. Such collective functional alterations consequently helped improve methane production efficiency and reaction stability. *R. flavefaciens* addition was associated with enhanced potential for synergistic interactions among the microbial populations, increased redox buffering capacity of the biofilm, and improved LCFA degradation and methane conversion efficiency.

4. Conclusions

The results of this study suggest that *R. flavefaciens* addition could improve anaerobic digestion performance toward model LCFA substrates. Under conditions containing ULCFAs and their inhibitory effects, 1% (*v*/*v*) addition of *R. flavefaciens* increased cumulative methane production by 270.9% and 186.0%, respectively. Notably, the 270.9% increase observed in the ULCFAs system represents a recovery from a crashed baseline, whereas the 186.0% improvement was obtained under the MLCFAs condition without such severe initial inhibitory pressure. *R. flavefaciens* addition accelerated acetate formation and prevented propionic acid accumulation. Metagenomic analysis revealed increased relative abundance of β-oxidation-related genes (*fadD*, *ACADS/bcd*, and *fadB*) and acetate-utilising methanogenesis genes (*acsC* and *cdhE*), concurrent with modest increases in the abundance of *Syntrophomonas* and *Methanosarcina*. Enhanced methanogenesis correlated with increased functional microbial abundance of *Xiashengella* and *Methanosarcina*. Finally, the observed correlations between specific taxa and enhanced performance should be interpreted cautiously given the inherent functional redundancy of anaerobic microbiomes. CAZymes prediction and species contribution analysis further indicated that *R. flavefaciens* addition enhanced functional potentials for GTs, CE4, and AA6 in the reaction, potentially aiding microbial polysaccharide synthesis, cell-wall structural remodelling, and redox detoxification regulation. These functional shifts are consistent with broader microbial

community adaptation, potentially supporting biofilm formation and improved system resilience under LCFA inhibition. Overall, *R. flavefaciens* addition appeared to alleviate LCFA inhibition, potentially reflecting enhanced substrate activation and mutualistic metabolic synergy, offering a potential biological strategy for stable and efficient anaerobic digestion of LCFA-rich substrates such as high-lipid waste.

Even so, these results are preliminary, as all experiments were performed in batch reactors; continuous-flow industrial digesters may experience microbial washout and dynamic LCFA accumulation that could alter bioaugmentation performance. Furthermore, only a single strain dosage gradient was tested without direct quantitative measurement of functional enzymes, leaving the system's scalability, long-term stability and in situ metabolic activity unvalidated. Apart from experimental constraints, osmotic pressure may influence the performance of *R. flavefaciens*. Although it was not the focus of the present study, its potential effects should be considered in follow-up research and practical application. When moving toward real-world implementation, beyond the above-mentioned research-scale limitations, multiple real-world barriers also hinder field deployment. Practical full-scale application is further constrained by the prohibitive cost of 1% v/v pure laboratory-cultivated DSM 25089. Although on-site enrichment using local waste substrates may reduce inoculum expenditure, industrial cultivation-dosing costs and ecological risks such as displacement of indigenous microbiota by exogenous strains remain to be assessed.

Therefore, future work should implement continuous-flow assays with multiple inoculum gradients and real-waste substrates, combined with enzyme activity determination and economic evaluation, to fill these research gaps and further verify the practical potential of this bioaugmentation strategy.

Author Contributions: C.W., J.L., S.W., Z.G., C.L. jointly contributed to the study conception and design. C.W. was responsible for investigation, conceptualization, experiment implementation, data col-lection, formal analysis, and original draft writing. C.L. acquired funding, supervised the research, and revised the manuscript. J.L. contributed to data analysis and experiment conduction. Z.G. provided guidance on experimental design. All authors have read and agreed to the published version of the manuscript.

Funding: This research was funded by Petroleum Management Bureau Co., Ltd. (Daqing, China) (No. dqc-2021-qt-ky-001), Heilongjiang Bayi Agricultural University Natural Science Talent Support Plan (No. ZRCQC202005), Heilongjiang Bayi Agricultural University Talent Research Initiation Plan (No. XYB202001) and Heilongjiang Bayi Agricultural University Natural Science Talent Support Program (No. ZRCPY202206).

Informed Consent Statement: Ethical approval was not required for this study as it did not involve human or animal subjects.

Data Availability Statement: All data generated or analysed during this study are included in this published article and are available from the corresponding author upon reasonable request.

Acknowledgments: We are deeply grateful to Chenxi Li for her dedicated supervision, generous funding support, and meticulous revision of this manuscript. We also thank Zhanbin Guo for his professional guidance on the experimental design. Funding support was provided by the Petroleum Management Bureau Co., Ltd. (Daqing, China) (No. dqc-2021-qt-ky-001), the Heilongjiang Bayi Agricultural University Natural Science Talent Support Plan (No. ZRCQC202005), the Heilongjiang Bayi Agricultural University Talent Research Initiation Plan (No. XYB2020001), and the Heilongjiang Bayi Agricultural University Natural Science Talent Support Program (No. ZRCPY202206).

Conflicts of Interest: The authors declare that this study received funding from Petroleum Management Bureau Co., Ltd. The funder was not involved in the study design, collection, analysis, interpretation of data, the writing of this article or the decision to submit it for publication.

Abbreviations

The following abbreviations are used in this manuscript:

LCFAs	Long Chain Fatty Acids
ULCFAs	Unsaturated Long Chain Fatty Acids
MLCFAs	Mixed Long Chain Fatty Acids
v/*v*	Volume per Volume (concentration measure)
H_2	Molecular Hydrogen
fadD	Acyl-CoA synthetase (LCFA activation)
ACADs/bcd	Acyl-CoA dehydrogenases/Butyryl-CoA dehydrogenase (β-oxidation enzymes)
fadB	Fatty Acid Oxidation Complex Subunit B
ECI1_2	Enoyl CoA isomerase (ULCFA isomerization)
cdhE	CO dehydrogenase/acetyl CoA synthase subunit (acetate cleavage)
frhB	F420 reducing hydrogenase (hydrogenotrophic methanogenesis)
mgsC	Methylamine—glutamate N-methyltransferase subunit C (methanogenesis pathway)
hdrB2	Heterodisulfide reductase (electron transport in methanogenesis)
mtrA	Methyl H4MPT: coenzyme M methyltransferase (electron transport)
fwdE/fmdE	Formylmethanofuran dehydrogenase subunit E
mer	5,10-Methylenetetrahydromethanopterin reductase
CAZymes	Carbohydrate Active Enzymes (general category)
GHs (e.g., GH2)	Glycoside Hydrolases (polysaccharide hydrolysis)
CEs (e.g., CE4, CE15)	Carbohydrate Esterases (deacetylation, side chain modification)
AAs (e.g., AA6)	Auxiliary Activity enzymes (oxidative/detoxification functions)
GTs (GT2, GT4)	Glycosyltransferases (polysaccharide backbone synthesis; enriched under *R. flavefaciens* addition)
β-oxidation	Metabolic pathway breaking down fatty acids
TS	Total Solids
VS	Volatile Solids
VS/TS	Ratio of Volatile Solids to Total Solids
SCOD	Soluble Chemical Oxygen Demand
AN	Ammonium Nitrogen
VFA/VFAs	Volatile Fatty Acid(s)
pH	Potential of Hydrogen
rpm	Revolutions Per Minute (centrifugation speed)
GC	Gas Chromatography
TCD	Thermal Conductivity Detector
MS 13X	Molecular Sieve Column (gas chromatography)
TG 16G	Centrifuge model (Kecheng Instruments, China)
KEGG	Kyoto Encyclopedia of Genes and Genomes
CAZy	Carbohydrate Active enZYmes Database
CFU	Colony Forming Units (measure of viable bacterial cells)
DSM	Deutsche Sammlung von Mikroorganismen (German Collection of Microorganisms, culture reference)
Chao1	Species richness estimator
Simpson index	Diversity/evenness index
Coverage index	Sequencing depth/representativeness
PCoA	Principal Coordinates Analysis (community structure visualisation)
Mantel test	Correlation between distance matrices
Pearson correlation	Linear correlation coefficient

Wilcoxon rank-sum test	Non-parametric test for two independent samples
SPSS	Statistical Package for the Social Sciences
OriginPro	OriginLab's data analysis and graphing software
U, U + 0.1R, U + 0.5R, U + 1R	ULCFA substrate + varying *R. flavefaciens* inoculum
M, M + 0.1R, M + 0.5R, M + 1R	MLCFA substrate + varying *R. flavefaciens* inoculum
K	Control group (no LCFA added)
U_7	ULCFA control
UR_7	ULCFA + *R. flavefaciens* (1% inoculum)
M_7	MLCFA control
MR_7	MLCFA + *R. flavefaciens* (1% inoculum)
M(t)	Methane yield as a function of time
P	Maximum methane potential
Rmax	Maximum methane generation rate
λ	Lag period

References

1. Duan, Y.; Wang, Z.; Ganeshan, P.; Sar, T.; Xu, S.; Rajendran, K.; Sindhu, R.; Binod, P.; Pandey, A.; Zhang, Z.; et al. Anaerobic Digestion in Global Bio-Energy Production for Sustainable Bioeconomy: Potential and Research Challenges. *Renew. Sustain. Energy Rev.* **2025**, *208*, 114985. [CrossRef]
2. Li, C.; Champagne, P.; Anderson, B.C. Evaluating and Modeling Biogas Production from Municipal Fat, Oil, and Grease and Synthetic Kitchen Waste in Anaerobic Co-Digestions. *Bioresour. Technol.* **2011**, *102*, 9471–9480. [CrossRef] [PubMed]
3. Abomohra, A.; Faisal, S.; Ebaid, R.; Huang, J.; Wang, Q.; Elsayed, M. Recent Advances in Anaerobic Digestion of Lipid-Rich Waste: Challenges and Potential of Seaweeds to Mitigate the Inhibitory Effect. *Chem. Eng. J.* **2022**, *449*, 137829. [CrossRef]
4. Tian, H.; Karachalios, P.; Angelidaki, I.; Fotidis, I.A. A Proposed Mechanism for the Ammonia-LCFA Synergetic Co-Inhibition Effect on Anaerobic Digestion Process. *Chem. Eng. J.* **2018**, *349*, 574–580. [CrossRef]
5. Zonta, Ž.; Alves, M.M.; Flotats, X.; Palatsi, J. Modelling Inhibitory Effects of Long Chain Fatty Acids in the Anaerobic Digestion Process. *Water Res.* **2013**, *47*, 1369–1380. [CrossRef] [PubMed]
6. Elsamadony, M.; Mostafa, A.; Fujii, M.; Tawfik, A.; Pant, D. Advances towards Understanding Long Chain Fatty Acids-Induced Inhibition and Overcoming Strategies for Efficient Anaerobic Digestion Process. *Water Res.* **2021**, *190*, 116732. [CrossRef] [PubMed]
7. Cirne, D.G.; Björnsson, L.; Alves, M.; Mattiasson, B. Effects of Bioaugmentation by an Anaerobic Lipolytic Bacterium on Anaerobic Digestion of Lipid-rich Waste. *J. Chem. Technol. Biotechnol.* **2006**, *81*, 1745–1752. [CrossRef]
8. Cavaleiro, A.J.; Sousa, D.Z.; Alves, M.M. Methane Production from Oleate: Assessing the Bioaugmentation Potential of Syntrophomonas zehnderi. *Water Res.* **2010**, *44*, 4940–4947. [CrossRef] [PubMed]
9. Dar, R.A.; Dai, B.; Tsui, T.-H.; Zhang, X.; Zhang, D.; Zhou, P.; Liu, R.; Zhang, L. Bioaugmentation with a Lipid-Degrading Bacterial Culture to Enhance Methane Production from Food Waste Anaerobic Digestion: Effect on Process Performance, Microbial Dynamics, and Lipid Metabolism. *Chem. Eng. J.* **2025**, *518*, 164539. [CrossRef]
10. Basak, B.; Tanpure, R.S.; Ahn, H.-J.; Ahn, Y.; Choi, K.-W.; Jang, M.; Kim, J.R.; Oh, S.-U.; Jeon, B.-H. Functional Microbiota Reconstruction Using Acclimatized Consortium and Trace Metal Supplementation Facilitates Process Recovery in Organic-Overloaded Anaerobic Digesters. *Chem. Eng. J.* **2025**, *512*, 162775. [CrossRef]
11. Israeli-Ruimy, V.; Bule, P.; Jindou, S.; Dassa, B.; Moraïs, S.; Borovok, I.; Barak, Y.; Slutzki, M.; Hamberg, Y.; Cardoso, V.; et al. Complexity of the Ruminococcus Flavefaciens FD-1 Cellulosome Reflects an Expansion of Family-Related Protein-Protein Interactions. *Sci. Rep.* **2017**, *7*, 42355. [CrossRef] [PubMed]
12. Brulc, J.M.; Yeoman, C.J.; Wilson, M.K.; Berg Miller, M.E.; Jeraldo, P.; Jindou, S.; Goldenfeld, N.; Flint, H.J.; Lamed, R.; Borovok, I.; et al. Cellulosomics, a Gene-Centric Approach to Investigating the Intraspecific Diversity and Adaptation of Ruminococcus Flavefaciens within the Rumen. *PLoS ONE* **2011**, *6*, e25329. [CrossRef] [PubMed]
13. Yeoman, C.J.; Fields, C.J.; Lepercq, P.; Ruiz, P.; Forano, E.; White, B.A.; Mosoni, P. In Vivo Competitions between Fibrobacter Succinogenes, Ruminococcus Flavefaciens, and Ruminoccus Albus in a Gnotobiotic Sheep Model Revealed by Multi-Omic Analyses. *MBio* **2021**, *12*, e03533-20. [CrossRef] [PubMed]
14. Latham, M.J.; Wolin, M.J. Fermentation of Cellulose by Ruminococcus Flavefaciens in the Presence and Absence of Methanobacterium Ruminantium. *Appl. Environ. Microbiol.* **1977**, *34*, 297–301. [CrossRef] [PubMed]
15. Weimer, P.J. Degradation of Cellulose and Hemicellulose by Ruminal Microorganisms. *Microorganisms* **2022**, *10*, 2345. [CrossRef] [PubMed]

16. Usman, M.; Salama, E.-S.; Arif, M.; Jeon, B.-H.; Li, X. Determination of the Inhibitory Concentration Level of Fat, Oil, and Grease (FOG) towards Bacterial and Archaeal Communities in Anaerobic Digestion. *Renew. Sustain. Energy Rev.* **2020**, *131*, 110032. [CrossRef]
17. Holliger, C.; Alves, M.; Andrade, D.; Angelidaki, I.; Astals, S.; Baier, U.; Bougrier, C.; Buffière, P.; Carballa, M.; De Wilde, V.; et al. Towards a Standardization of Biomethane Potential Tests. *Water Sci. Technol.* **2016**, *74*, 2515–2522. [CrossRef] [PubMed]
18. Raper, E.; Stephenson, T.; Anderson, D.R.; Fisher, R.; Soares, A. Industrial Wastewater Treatment through Bioaugmentation. *Process Saf. Environ. Prot.* **2018**, *118*, 178–187. [CrossRef]
19. Wu, L.-J.; Hao, Z.-W.; Ye, F.; Yang, F.; Lyu, Y.-K. Oil in Food Waste to Methane by Anaerobic Digestion: Co-Effects of Mixing Intensity and Long Chain Fatty Acid Loading. *Process Saf. Environ. Prot.* **2024**, *190*, 598–605. [CrossRef]
20. Sousa, D.Z.; Salvador, A.F.; Ramos, J.; Guedes, A.P.; Barbosa, S.; Stams, A.J.M.; Alves, M.M.; Pereira, M.A. Activity and Viability of Methanogens in Anaerobic Digestion of Unsaturated and Saturated Long-Chain Fatty Acids. *Appl. Environ. Microbiol.* **2013**, *79*, 4239–4245. [CrossRef] [PubMed]
21. Lalman, J.A.; Bagley, D.M. Anaerobic Degradation and Methanogenic Inhibitory Effects of Oleic and Stearic Acids. *Water Res.* **2001**, *35*, 2975–2983. [CrossRef] [PubMed]
22. De Vrieze, J.; Pinto, A.J.; Sloan, W.T.; Ijaz, U.Z. The Active Microbial Community More Accurately Reflects the Anaerobic Digestion Process: 16S rRNA (Gene) Sequencing as a Predictive Tool. *Microbiome* **2018**, *6*, 63. [CrossRef] [PubMed]
23. Ostos, I.; Flórez-Pardo, L.M.; Camargo, C. A Metagenomic Approach to Demystify the Anaerobic Digestion Black Box and Achieve Higher Biogas Yield: A Review. *Front. Microbiol.* **2024**, *15*, 1437098. [CrossRef] [PubMed]
24. Pereira, M.A.; Pires, O.C.; Mota, M.; Alves, M.M. Anaerobic Degradation of Oleic Acid by Suspended and Granular Sludge: Identification of Palmitic Acid as a Key Intermediate. *Water Sci. Technol.* **2002**, *45*, 139–144. [CrossRef]
25. Jiang, Y.; McAdam, E.; Zhang, Y.; Heaven, S.; Banks, C.; Longhurst, P. Ammonia Inhibition and Toxicity in Anaerobic Digestion: A Critical Review. *J. Water Process Eng.* **2019**, *32*, 100899. [CrossRef]
26. Town, J.R.; Dumonceaux, T.J. Laboratory-Scale Bioaugmentation Relieves Acetate Accumulation and Stimulates Methane Production in Stalled Anaerobic Digesters. *Appl. Microbiol. Biotechnol.* **2016**, *100*, 1009–1017. [CrossRef] [PubMed]
27. Walls, L.E.; Otoupal, P.; Ledesma-Amaro, R.; Velasquez-Orta, S.B.; Gladden, J.M.; Rios-Solis, L. Bioconversion of Cellulose into Bisabolene Using Ruminococcus Flavefaciens and Rhodosporidium Toruloides. *Bioresour. Technol.* **2023**, *368*, 128216. [CrossRef] [PubMed]
28. Čater, M.; Fanedl, L.; Malovrh, Š.; Marinšek Logar, R. Biogas Production from Brewery Spent Grain Enhanced by Bioaugmentation with Hydrolytic Anaerobic Bacteria. *Bioresour. Technol.* **2015**, *186*, 261–269. [CrossRef] [PubMed]
29. Ozbayram, E.G.; Akyol, Ç.; Ince, B.; Karakoç, C.; Ince, O. Rumen Bacteria at Work: Bioaugmentation Strategies to Enhance Biogas Production from Cow Manure. *J. Appl. Microbiol.* **2018**, *124*, 491–502. [CrossRef] [PubMed]
30. Mani, A.M.M.; Al Araji, R.; Ghazi, H. Activated Charcoal Derivated from Biochar as a Feed Additive for Goats: A Ruminal Analysis. *AVM* **2025**, *18*, 61–75. [CrossRef]
31. Huang, H.-J.; Zhang, X.; Sun, X.-W.; Chen, B.; Li, X.-T.; Zhou, N.; Abdugheni, R.; Cheng, Q.-Y.; Zhang, T.-J.; Liu, Y.; et al. Xiashengella Succiniciproducens Gen. Nov., Sp. Nov., a Succinate-Producing Bacterium Isolated from an Anaerobic Digestion Tank in the Family Marinilabiliaceae of the Order Bacteroidales. *Arch. Microbiol.* **2024**, *206*, 141. [CrossRef] [PubMed]
32. Kim, H.W.; Oh, W.; Liu, P.; Su, X.; Mackie, R.I. Glucose-Driven Uncoupling of Methanogenesis from Acidogenesis to Generate Carboxylates in Anaerobic Digestion: Insights into Microbial Dynamics and Operational Parameters. *Biomass Bioenergy* **2026**, *209*, 108990. [CrossRef]
33. Ziels, R.M.; Sousa, D.Z.; Stensel, H.D.; Beck, D.A.C. DNA-SIP Based Genome-Centric Metagenomics Identifies Key Long-Chain Fatty Acid-Degrading Populations in Anaerobic Digesters with Different Feeding Frequencies. *ISME J.* **2018**, *12*, 112–123. [CrossRef] [PubMed]
34. Louca, S.; Polz, M.F.; Mazel, F.; Albright, M.B.N.; Huber, J.A.; O'Connor, M.I.; Ackermann, M.; Hahn, A.S.; Srivastava, D.S.; Crowe, S.A.; et al. Function and Functional Redundancy in Microbial Systems. *Nat. Ecol. Evol.* **2018**, *2*, 936–943. [CrossRef] [PubMed]
35. Jensen, M.B.; De Jonge, N.; Dolriis, M.D.; Kragelund, C.; Fischer, C.H.; Eskesen, M.R.; Noer, K.; Møller, H.B.; Ottosen, L.D.M.; Nielsen, J.L.; et al. Cellulolytic and Xylanolytic Microbial Communities Associated with Lignocellulose-Rich Wheat Straw Degradation in Anaerobic Digestion. *Front. Microbiol.* **2021**, *12*, 645174. [CrossRef] [PubMed]
36. Amha, Y.M.; Anwar, M.Z.; Brower, A.; Jacobsen, C.S.; Stadler, L.B.; Webster, T.M.; Smith, A.L. Inhibition of Anaerobic Digestion Processes: Applications of Molecular Tools. *Bioresour. Technol.* **2018**, *247*, 999–1014. [CrossRef] [PubMed]
37. Wang, L.; Shan, X.; Xu, Y.; Xi, Q.; Jiang, H.; Li, X. Analysis of Mechanisms for Electron Uptake by Methanothrix Harundinacea 6Ac During Direct Interspecies Electron Transfer. *Int. J. Mol. Sci.* **2025**, *26*, 4195. [CrossRef] [PubMed]
38. Alshareef, S.A. Metabolic Analysis of the CAZy Class Glycosyltransferases in Rhizospheric Soil Fungiome of the Plant Species Moringa Oleifera. *Saudi J. Biol. Sci.* **2024**, *31*, 103956. [CrossRef] [PubMed]
39. Wang, H.; Fotidis, I.A.; Angelidaki, I. Ammonia Effect on Hydrogenotrophic Methanogens and Syntrophic Acetate-Oxidizing Bacteria. *FEMS Microbiol. Ecol.* **2015**, *91*, fiv130. [CrossRef] [PubMed]

40. Kouzuma, A.; Tsutsumi, M.; Ishii, S.; Ueno, Y.; Abe, T.; Watanabe, K. Non-Autotrophic Methanogens Dominate in Anaerobic Digesters. *Sci. Rep.* **2017**, *7*, 1510. [CrossRef] [PubMed]
41. Liu, Y.; Xi, Y.; Li, Q.; Dzakpasu, M.; Chen, R.; Li, Y.-Y. Biokinetic and Microbial Insights into Regulatory Mechanisms of Long-Chain Fatty Acid Degradation during Food Waste-Lipid Co-Digestion within Anaerobic Membrane Bioreactor. *Bioresour. Technol.* **2024**, *408*, 131223. [CrossRef] [PubMed]
42. Aragunde, H.; Biarnés, X.; Planas, A. Substrate Recognition and Specificity of Chitin Deacetylases and Related Family 4 Carbohydrate Esterases. *Int. J. Mol. Sci.* **2018**, *19*, 412. [CrossRef] [PubMed]

Disclaimer/Publisher's Note: The statements, opinions and data contained in all publications are solely those of the individual author(s) and contributor(s) and not of MDPI and/or the editor(s). MDPI and/or the editor(s) disclaim responsibility for any injury to people or property resulting from any ideas, methods, instructions or products referred to in the content.